TOPICAL REVIEW

Acta Cryst. (1999). B**55**, 811–829

Metastructures: homeomorphisms between complex inorganic structures and three-dimensional nets

M. Schindler,[a]* F. C. Hawthorne[a] and W. H. Baur[b]

[a]*Department of Geological Sciences, University of Manitoba, Winnipeg, Manitoba, Canada R3T 2N2, and* [b]*Department of Geophysical Sciences, University of Chicago, Chicago, IL 60637, USA.*
E-mail: schindl0@cc.umanitoba.ca

(*Received 27 January 1999; accepted 7 September 1999*)

Abstract

We propose a general approach to nets and structures in which vertices represent stereochemically significant groups or clusters of atoms, and edges represent the linkage between these groups. Vertices may be single atoms, dimers, coordination polyhedra, clusters of atoms or clusters of coordination polyhedra; edges may be single chemical bonds or sets of several chemical bonds. Thus, a single net may be the basis for a family of structures that are homeomorphic to that net. The coordination of polyhedra or units around a vertex is visualized by connecting the *centres* of the atoms or groups at the vertices connected with the central vertex. Thus, the concept of coordination number is extended to include coordinating *groups*. We name a net after a homeomorphic simple structure-type for which there is a one-to-one correspondence between the vertices of the net and specific atoms of the structure, and between the edges of the net and the chemical bonds. We term the resulting more complex structures *metastructures* in order to distinguish them from their corresponding simple structure-types. Individual metastructures are referred to as *alpha structures* similar to a particular simple type. Thus, the open complex framework of $[V_5O_9(PO_4)_2]$ composition in microporous $Na_v[((V^{4+}_{4-w}V^{5+}_{1+w})O_9)(PO_4)_2]\cdot(PO_4)_x\cdot(OH)_y\cdot zH_2O$ is an α-NbO structure based on the simple net that is homeomorphic to NbO. This approach is effective in hierarchically classifying both simple close-packed structures and very complicated microporous structures.

Michael Schindler studied mineralogy in Frankfurt am Main, where he obtained his D.Phil.nat. in 1997 examining vanadium/phosphate/water systems at 200°C under hydrothermal conditions. Here he synthesized and characterized a new class of microporous vanadium phosphates. His scientific interests include crystal chemistry of minerals and inorganic solids, substitution processes in rock-forming minerals, topological descriptions of inorganic materials and examinations of mineral- and inorganic-aqueous systems under different conditions.

Frank C. Hawthorne did his Ph.D. at McMaster University, working on the crystal chemistry of amphiboles. He is Distinguished Professor of Crystallography and Mineralogy in the Department of Geological Sciences at the University of Manitoba. Interests include topological and electronic aspects of crystal structures, solution of unknown mineral structures, all forms of spectroscopy, microbeam analysis, applications of the Rietveld method, crystal chemistry and ordering in complex mineral structures.

Werner H. Baur's scientific project is the study of variations in geometry and symmetry of crystal structures under varying chemical conditions. He approaches this experimentally by studying crystal structures of minerals and inorganic compounds, especially zeolites, or by computer simulations of structures and electrostatic energy calculations, or by empirical syntheses of crystal chemical data. The last two topics include concepts pioneered by him. He obtained the D.rer.nat. 1956 in Göttingen working on rutiles.

1. Introduction

Complex inorganic crystal structures are notoriously difficult to visualize and, from early on, crystallographers have used a variety of methods to comprehend their architecture. At first, the similarity of arrangements of anions to close packings was emphasized, as was done by Bragg & Brown (1926) for olivine. It was soon recognized that the centres of anions adjacent to a cation outline a simple polyhedron. The arrangements of these coordination polyhedra are easier to visualize than arrangements of numerous individual atoms, as shown by Pauling & Sturdivant (1928) in their study of brookite. In a series of papers on the 'Geometric basis of crystal chemistry', Wells (1954)

pioneered another way to describe the topology and geometry of complex inorganic crystal structures, viewing them as three-dimensional nets in which the edges correspond to chemical bonds between atoms located at the vertices. These studies were summarized and extended by Wells (1977, 1979) who derived numerous simple three-dimensional nets of high symmetry with three and four edges incident at a vertex. For many of his nets, Wells identified crystal structures with the same bond topology. Usually, he considered cases in which there is a one-to-one correspondence between atoms and vertices, and bonds and edges. However, for the fibrous zeolites he derived nets of a higher order of simplification: he viewed the 'fibrous' chains, consisting of a repeat of five tetrahedra, as one unit. The connections between these chain units were considered as comprising the net (Wells, 1977, p. 160). Owing to the importance of framework silicates, particularly the zeolites, several groups have studied four-connected three-dimensional nets (Smith, 1977, 1978, 1979; Smith & Rinaldi, 1962; Han & Smith, 1999; Akporiaye, 1994; O'Keeffe, 1995). This has led to a rational classification of such nets, has allowed the prediction of new crystal structures and has simplified the description of known structures.

Another way to systematize inorganic structure types is to approach them hierarchically. Minerals have been classified according to their degree of polymerization of coordination polyhedra: silicates (Bragg, 1930; Zoltai, 1960; Liebau, 1985), borates (Hawthorne *et al.*, 1996), phosphates (Moore, 1984) and aluminofluorides (Hawthorne, 1984). However, many of these hierarchical schemes focus on specific chemical classes of compounds and most are not easily adapted to other classes. General observations on families of complex structures based on different arrangements of basic structural units have been made by Hawthorne (1979, 1990, 1994, 1997, for example) and Moore (1974, 1975, for example). These studies focused on structures with triangles, tetrahedra and octahedra as principal components of the structural units. For zeolites, Meier (1968) derived Secondary Buildings Units or SBUs, clusters of linked tetrahedra from which zeolite frameworks can be constructed, subject to the constraint that an entire framework consists only of one type of SBU.

2. Description of very complicated structures

In the last 10 years, one of the goals of materials science has been the creation of micro-, meso- and nanoporous materials for industrial applications such as shape-selective catalysis. In this context, a large number of inorganic crystal structures with phosphate, arsenate, cyanide and chalcogenide groups have been synthesized. Bowes & Ozin (1996) reviewed the topologies of cyanide and chalcogenide structures in terms of their dimensions, linking units, open channels and, if existing, their interpenetrating nets. Iwamoto *et al.* (1997) showed similarities between certain cyanide structures and di-, group, chain, ring, layer and framework silicates. Furthermore, they identified cyanide compounds with nets analogous to well known simple structure types such as PtS, cuprite, pyrite and rutile. Schindler & Baur (1997) showed that the topologies of certain complex vanadium phosphates correspond to those of the aluminosilicates sodalite and zeolite rho: they contain functional groups, such as $[V_5O_9(PO_4)_2]$, in place of single four rings (S4R), $[Si_4O_{12}]$, within the topologies of sodalite and zeolite rho. They termed the resulting complex vanadium-phosphate topologies *α-topologies*, in order to distinguish them from the well known aluminosilicate structures: in a net of an *α-structure*, we do not have a one-to-one correspondence of single atoms and bonds with vertices and edges; their similarity to the basic nets is at the level of larger groups of polyhedra. Schindler & Baur (1997) also showed that, rather than the $[V_5O_9(PO_4)_2]$ group, other groups of different chemical composition and geometry (*e.g.* $[Mo_4O_8(PO_4)_2]$) can occur with the *α-sodalite* topology. Yaghi *et al.* (1998) reviewed the assembly of materials from molecular building blocks. In their examples, the molecular building blocks were metal-sulfide clusters (*e.g.* $[Ge_4S_{10}]$, $[MnS_4]$) and organic molecules with transition-metal ions. They described their functionality, shape, size, various synthesis strategies and the modular porous networks that they form.

Batten & Robson (1998) reviewed the occurrence of interpenetrating nets in organic and inorganic structures. They classified chemically different structures according to the underlying net and they described the type of clusters or groups residing at the nodes of the corresponding nets.

Robson *et al.* (1992) and Carlucci & co-workers (*e.g.* Carlucci *et al.*, 1995, 1997) showed topological relations between several simple two- and three-dimensional nets and polymeric coordination compounds. These polymeric coordination compounds include

(*a*) [2]-coordinated linear bidentate ligands, which connect vertices occupied by metallic cations,

(*b*) polydentate ligands connecting alternatively metallic and organic centres and

(*c*) linear Ag^I and Cu^I coordinations as simple spacers or connectors for ligands.

Excellent review articles concerning compounds containing primarily cyano groups with organic coordination groups on nodes of two- and three-dimensional nets are given by Iwamoto (1996*a*,*b*) and Robson (1996).

Here, we list only complex structures which can be described as the insertion of inorganic polyhedral groups or clusters at vertices of simple three-dimensional nets. We combine the approach of Wells (1977, 1979) and Smith (1977, 1978, 1979) with the hierarchical classifications of Moore (1984) and Hawthorne (1985, 1986, 1990) by considering complex compounds as nets

in which the vertices can be occupied by clusters of polyhedra as well as by individual atoms.

3. Nets and topology

Wells (1979) defined a three-dimensional net as a system of connected nodes which extends indefinitely in three dimensions and in which some pattern of nodes repeats periodically in three noncoplanar directions. Two nets are topologically identical when they are homeomorphic. A homeomorphism or topological transformation, φ, is a mapping of a net onto itself if and only if there is a one-to-one correspondence of vertices and edges. A one-to-one correspondence means that any two vertices P and Q of two nets map onto each other ($\varphi P = Q$). This implies that an inverse transformation exists, φ^{-1}, which maps $\varphi^{-1}(Q)$ onto P if and only if φP is equal to Q. The composition of two homeomorphisms and the inverse of a homeomorphism are all homeomorphisms, and thus topological equivalence is an equivalence relation.

A net is an infinite graph in which the degree of a vertex, v, is defined as the number of edges incident at v. If one graph can be obtained from another by the insertion of new vertices of degree two into its edges, then the two graphs are homeomorphic. In a colored graph, vertices are colored. The chromatic number, k, of a graph is defined as the number of colors which are possible when $k - 1$ colors are not possible. A two-chromatic graph is termed a bipartite graph when edges always connect vertices of different colors. A path is a continuous sequence of edges and a circuit is a closed path that begins and ends at the same vertex. Circuits which do not contain shorter paths along the circuit between any two vertices on the circuit are termed *fundamental circuits* or *rings* (O'Keeffe & Hyde, 1996). In a three-dimensional net, there are an infinitive number of circuits for each vertex, but only a finite number of rings.

Any two edges with a common vertex define an angle at that vertex. In a four-connected net, there are four edges, a, b, c and d, incident at any vertex of the net. A pair of edges (such as ab) define an angle at that vertex and there are six angles at each vertex. A net can be described by a Schläfli symbol which denotes the number of N-gons (n) in the shortest circuits around each node. For the diamond net (Fig. 1), the corresponding Schläfli symbol is 6^6, because there are six 6-gons in the shortest circuits around each node. O'Keeffe & Hyde (1996) used a long Schläfli symbol which describes all the rings at the angles around a vertex v. The long Schläfli symbol for the diamond net is $6_2{\cdot}6_2{\cdot}6_2{\cdot}6_2{\cdot}6_2{\cdot}6_2$ (note that the number of rings are given as subscripts) because there are two 6-rings around each angle. The symbols are arranged in corresponding pairs of opposing angles (*i.e.* those angles which do not have a common edge).

Following Wells (1979), it is convenient to name three-dimensional nets after simple structure types, such as diamond and NbO, because of the relation of the nets to the corresponding structures of these materials. The relation of a net to a simple structure is a homeomorphism, because there is a one-to-one correspondence between the vertices of the net and specific atoms of the structure, and between the edges of the net and the chemical bonds. In this paper, nets will be named after the corresponding structure types and the topologies will be described by long Schläfli symbols.

A six-valent vertex involves 15 angles, but three angles ($\sim 180^\circ$) are only included in circuits which contain shorter paths to vertices on the circuit and, therefore, are not listed in the long Schläfli symbol. In the same way, only 24 out of 28 angles around an eight-valent vertex are listed. For vertices with valences higher than four, the rings in the long Schläfli symbol are ordered with increasing ring size and the numbers of equivalent rings are shown as superscripts outside the square brackets (*e.g.* rutile $[4]^2{\cdot}[6_2]^2[6]^8/[4{\cdot}[6_2]^2]$).

4. A general approach

In most previous work, there has been complete one-to-one correspondence (*i.e.* homeomorphism) between a net and its corresponding structure. An important exception to this is the approach of Smith (1977) in the case of framework silicates (and chemical variants thereof), in which each four-connected vertex represents a tetrahedrally coordinated cation and each edge represents *two* T—O bonds and their linking anion. However, there is still a one-to-one correspondence between vertices and atoms, and between edges and

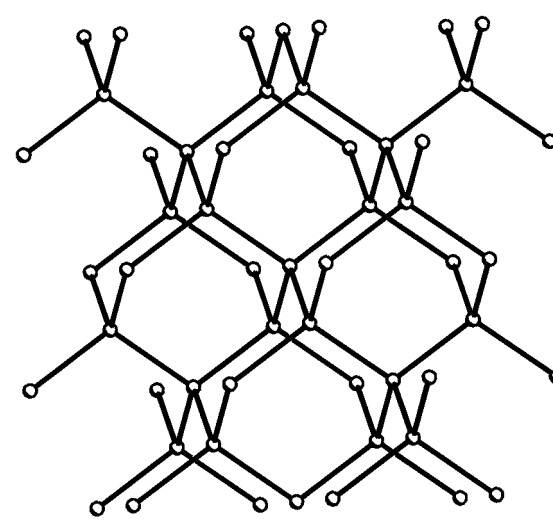

Fig. 1. The diamond net with four-connected vertices marked with white circles. The corresponding Schläfli symbol is 6^6 and the long Schläfli symbol is $6_2{\cdot}6_2{\cdot}6_2{\cdot}6_2{\cdot}6_2{\cdot}6_2$.

single bonds, as the anion is understood to be a divalent vertex on each edge of the net.

A somewhat different (more graph-theoretic) approach was taken by Hawthorne (1983). In a graph, a vertex can represent anything (*e.g.* an atom, a person, a cluster of atoms) and an edge can represent their interaction (*e.g.* a chemical bond, a relationship, linkage between clusters of atoms); this has the advantage that complexities in the interaction between vertices can be represented by multiple edges. This suggests a more general approach to nets and structures whereby vertices represent any stereochemically significant groups or clusters of atoms, and edges represent the linkage between these groups. Vertices may be single atoms, dimers, coordination polyhedra, clusters of atoms or clusters of coordination polyhedra; edges may be single chemical bonds or sets of several chemical bonds.

Vertices of different degree can be designated by different colors. A graph with vertices of two different degrees is a two-colored graph. In the two-colored graphs of this paper, the vertex with the higher degree is designated as a black vertex and the vertex with the lower degree is designated as a white vertex. We emphasize the chemical identities of the units at the black and white vertices by putting the atoms, polyhedra or groups in square brackets (*e.g.* $[V_5O_9]$) and listing them separately in the chemical composition.

The number of connections around the units at a vertex is equal to the degree of that vertex. The one-to-one correspondence between the vertices of a net and atoms, polyhedra or groups of polyhedra in a crystal structure, and between edges and linkages yields the number of connections of a unit at a vertex with atoms or groups at the adjacent vertices. The coordination polyhedra or units around the vertices can be tetrahedra, octahedra, square-planar units *etc.*, and they can be visualized by connecting the *centres* of the atoms or groups at the vertices with each other. We term the resulting more complex structures *metastructures* in order to distinguish them from the corresponding simple structure types and from the nets themselves. Individual metastructures are referred to as *alpha structures*, which correspond to a simple structure type: the open complex framework of $[V_5O_9(PO_4)_2]$ composition in microporous $Na_v[((V^{4+}_{4-w}V^{5+}_{1+w})O_9)(PO_4)_2]\cdot(PO_4)_x\cdot(OH)_y\cdot zH_2O$ is an α-NbO structure based on the simple net of bonds in NbO. Individual nets, the corresponding simple structure types and α-structures are homeomorphic. Homeomorphic structures retain the topology (but not necessarily the symmetry) of the underlying net.

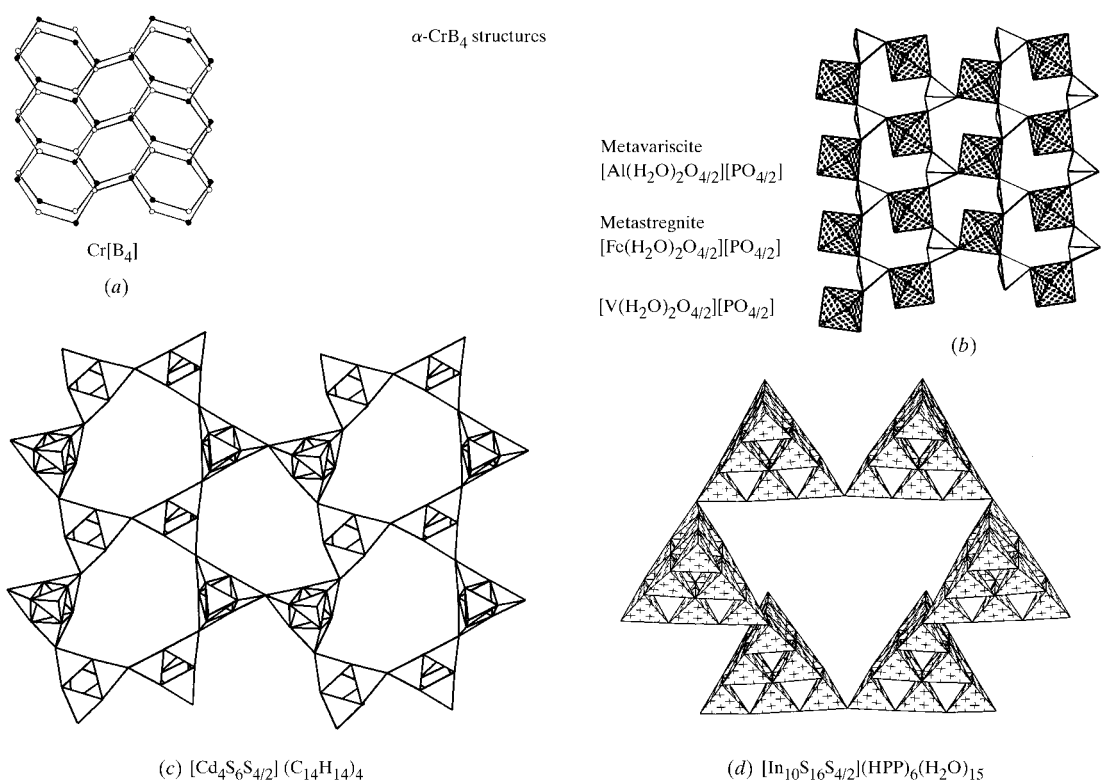

Fig. 2. (*a*) The CrB_4 net; the four-connected vertices are alternately occupied by dark and white circles. In the α-CrB_4 structure of metavariscite (*b*), the four-connected vertices are occupied by $[PO_{4/2}]$ or $[Al(H_2O)_2O_{4/2}]$, (*c*) in $[Cd_4S_6S_{4/2}](C_{14}H_{14})_4$ by $[Cd_4S_6S_{4/2}]$ adamantane groups and (*d*) in $In_{10}S_{18}(DPM)_3$ (ASU32) by $[In_{10}S_{16}S_{4/2}]$ tetrahedra.

4.1. *An example*

It is instructive to consider a net that is homeomorphic to the CrB_4 structure type. In CrB_4, B atoms coordinate to each other tetrahedrally and form a framework, and Cr atoms occupy the interstices. The earliest description of the corresponding three-dimensional net was given by Wells (1954, Fig. 2). He derived this, and other related nets, from systematically exploring up and down linkages from the two-dimensional 6^3 net. For the CrB_4-type net (Fig. 2*a*), the sequence of linkages within a six-ring is UDDUDD (U = up, D = down). The space group of highest symmetry for that net is *I*4/*mmm*. The short Schläfli symbol is 4.6^5 and the long symbol is $4{\cdot}6_2{\cdot}6{\cdot}6{\cdot}6{\cdot}6$. Smith (1977) showed that this net is homeomorphic to the aluminosilicate framework of metastable monoclinic $Ca[Al_2Si_2O_8]$ (Takéuchi *et al.*, 1973), where $[AlO_{4/2}]$ and $[SiO_{4/2}]$ tetrahedra reside at the four-connected vertices. Schindler *et al.* (1995) recognized that the structures of metavariscite $[Al(H_2O)_2(PO_4)]$ (Kniep & Mootz, 1973), metastrengite $[Fe(H_2O)_2(PO_4)]$ (Moore, 1966) and $[V(H_2O)_2(PO_4)]$ (Schindler *et al.*, 1995) are based on the same net. In metavariscite, each $M(H_2O)_2O_4$ octahedron (M = Fe, Al, V) shares four O atoms with four adjacent phosphate tetrahedra (Fig. 2*b*) and the bonded H_2O groups occur in the interstices of the framework. In the crystal structure of $[Cd_4S_6S_{4/2}](C_{14}H_{14})_4$ (Dance *et al.*, 1987), the adamantane-like $[Cd_4S_6S_{4/2}]$ groups occur at the vertices of the CrB_4 net (Fig. 2*c*). Recently, Li *et al.* (1999) reported the crystal structure of $In_{10}S_{18}(DPM)_3$ (ASU32, DPM = dipiperidanomethane) with $[In_{10}S_{16}S_{4/2}]$ (Fig. 2*d*) tetrahedra on the four-valent vertices.

Table 1. *Survey of α-CrB_4 structures, the groups at the vertices and the approximate magnification compared with the CrB_4 structure*

Compound	Groups at the vertices	Magnification
$Cr[B_4]$	[*B*]	1.0
$Ca[Si_2Al_2O_8]$	$[SiO_{4/2}]/[AlO_{4/2}]$	1.9
$[V(H_2O)_2PO_4]$	$[V(H_2O)O_{4/2}]/[PO_{4/2}]$	2.0
$[Cd_4S_8](C_{14}H_{14})_4$	$[CdS_6S_{4/2}]$	5.6
$[In_{10}S_{18}](DPM)_3$ (ASU32)	$[In_{10}S_{16}S_{4/2}]$	8.3

In this example, vertices can be occupied by such different chemical groups as [B], $[AlO_{4/2}]$, $[SiO_{4/2}]$, $[PO_{4/2}]$, $[Al(H_2O)_2O_{4/2}]$, $[Fe(H_2O)_2O_{4/2}]$, $[V(H_2O)_2O_{4/2}]$ $[Cd_4S_6S_{4/2}]$ and $[In_{10}S_{16}S_{4/2}]$ (Table 1, Fig. 2).

Tables 1–9 list the constituent groups at the vertices (when of different degrees: black and white vertices) and a very approximate magnification factor for comparison with the simple structure-type itself. The magnification shows how much the dimensions of the

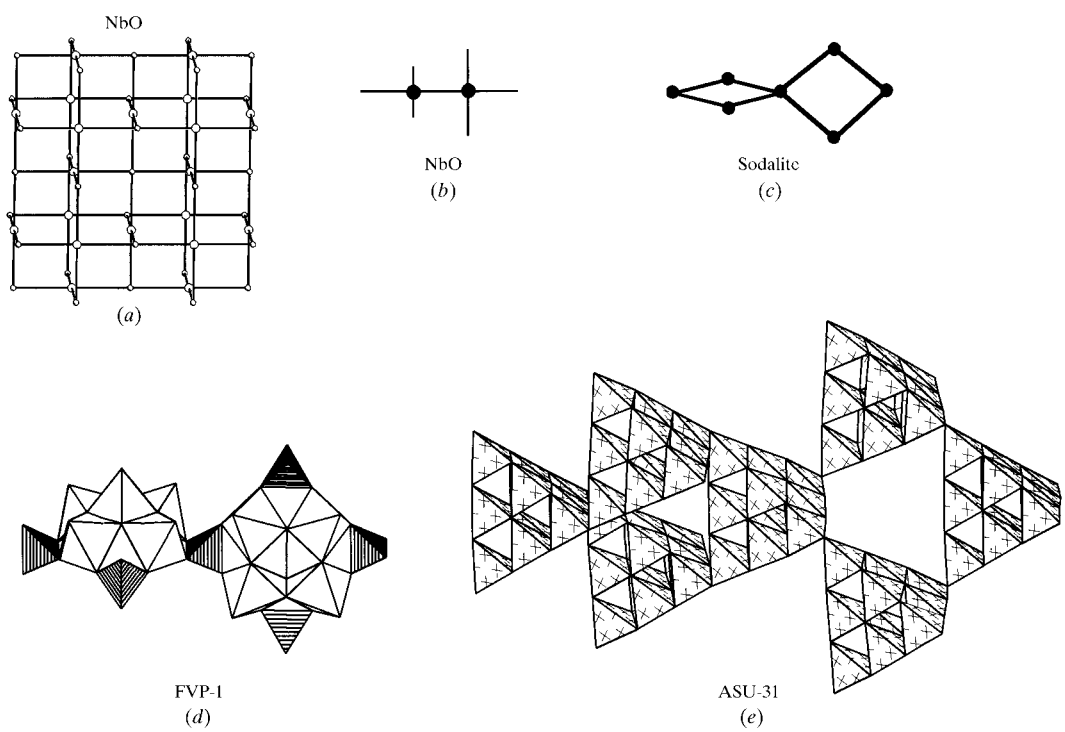

Fig. 3. (*a*) The NbO net and the different groups in structures with α-NbO topology. Whereas in (*b*) NbO, the vertices are occupied by two different atoms (Nb, large circles; O, small circles), in the α-structures, only one type of group is present at the vertices. (*c*) Two square-planar four-membered rings of the sodalite structure are shown as links between the central Si/Al atoms, and (*d*) two $[V_5O_9(PO_4)_{4/2}]$ and (*e*) two $[(In_{10}S_{16}S_{4/2})_4]$ units each are shown in a polyhedral representation.

Table 2. *Survey of α-NbO structures, the groups at the vertices and the approximate magnification compared with the NbO structure*

Compound	Groups at the vertices	Magnification
NbO	[Nb][O]	1
Sodalite: $Na_6[Al_6Si_6O_{24}]\cdot 2NaCl$	$[Si_2Al_2O_4O_{8/2}]$	2
$((CH_3)_4N)_{1.3}(H_3O)_{0.7}[Mo_4O_8(PO_4)_2]\cdot 2H_2O$	$[Mo_4O_8(PO_4)_{4/2}]$	3.4
Phosphovanadylite: (Ba,Ca,K,Na)[(V,Al)-$(O,OH)_8(PO_4)_2\cdot 12H_2O$	$[V_4O_8(PO_4)_{4/2}]$	3.4
$Na_v[((V^{4+}_{4-w}V^{5+}_{1+w})O_9)(PO_4)_2]\cdot(PO_4)_x\cdot(OH)_y\cdot zH_2O$ (FVP-1)	$[V_5O_9(PO_4)_{4/2}]$	3.8
$In_{10}S_{18}(HPP)_6(H_2O)_{15}$ (ASU31)	$[(In_{10}S_{16}S_{4/2})_4]$	8.1

Table 3. *Survey of α-NaCl structures, their groups (A and B) at the vertices and the approximate magnification compared with the NaCl structure*

Compound	Group *A*	Group *B*	Magnification
Halite: NaCl	[Na]	[Cl]	1
Pyrite: FeS_2	[Fe]	$[S_2]$	1
SiP_2O_7	$[SiO_{6/2}]$	$[OP_2O_{6/2}]$	1.3
$(H_{31}O_{14})[CdCu_2(CN)_7]$	$[Cd(CN)_{6/2}]$	$[CNCu_2(CN)_{6/2}]$	2.3
$AlPO_4$-16, $[Al_{20}P_{20}O_{80}]$	$[AlO_4P_4O_{12/2}]$	$[PO_4Al_4O_{12/2}]$	2.4
Zunyite: $[Si_5Al_{13}O_{20}(OH)_{14}F_4Cl]$	$[AlO_4Al_{12}O_{12/2}(OH)_{14}F_4]$	$[SiO_4Si_4O_{12/2}]$	2.5
Zeolite A: $Na_{12}[Al_{12}Si_{12}O_{12}O_{48}]\cdot 27H_2O$	$[Al_{12}Si_{12}O_{12}O_{24/2}]$	$[Al_{12}Si_{12}O_{12}O_{24/2}]$	4.4

Table 4. *Survey of α-ReO_3 structures, their groups at the black and white vertices, and the approximate magnification compared with the ReO_3 structure*

Compound	Group at the black vertices	Group at the white vertices	Magnification
ReO_3	[Re]	[O]	1
$Fe^{3+}(Fe^{3+}(CN)_6)$	$[Fe^{3+}]$	[CN]	1.4
Sulvanite: Cu_3VS_4	$[VS_4]$	[Cu]	1.4
Pharmacosiderite: $K[Fe_4(OH)_4(AsO_4)_3]\cdot 6H_2O$	$[Fe_4(OH)_4]$	$[AsO_4]$	2.1
Boracite: $Mg_3[B_4O(BO_4)_{6/2}]Cl$	$[OB_4]$	$[BO_4]$	2.3
$Rb_3[Zn_4O(PO_4)_3]\cdot 3.5\ H_2O$	$[OZn_4]$	$[PO_4]$	2.9
$Fe(NH_3)_6[Cu_8S(SbS_4)_3]$	$[SCu_8]$	$[SbS_4]$	3.4

metastructures increase as larger units occupy the vertices (black or white).

5. NbO ($6_2{\cdot}6_2{\cdot}6_2{\cdot}6_2{\cdot}8_2{\cdot}8_2$) and sodalite (4·4·6·6·6·6) nets and their metastructures

The crystal structure of NbO (Bowman *et al.*, 1966) can be interpreted as a defect structure of the NaCl structure type, with one quarter of the Nb and O sites vacant in an ordered fashion: $Nb_{0.75}O_{0.75}$ (Wells, 1984, p. 539). There are only three Nb and three O atoms in the unit cell; the sites at (0 0 0) and ($\frac{1}{2}$ $\frac{1}{2}$ $\frac{1}{2}$) remain vacant. The NaCl structure has space-group symmetry $Fm\bar{3}m$ with Wyckoff sites 4(*a*) and 4(*b*) occupied by Na and Cl, respectively. The NbO structure has space-group symmetry $Pm\bar{3}m$ with Nb and O occupying the 3(*c*) and 3(*d*) sites, respectively. In NbO, the Nb and O atoms

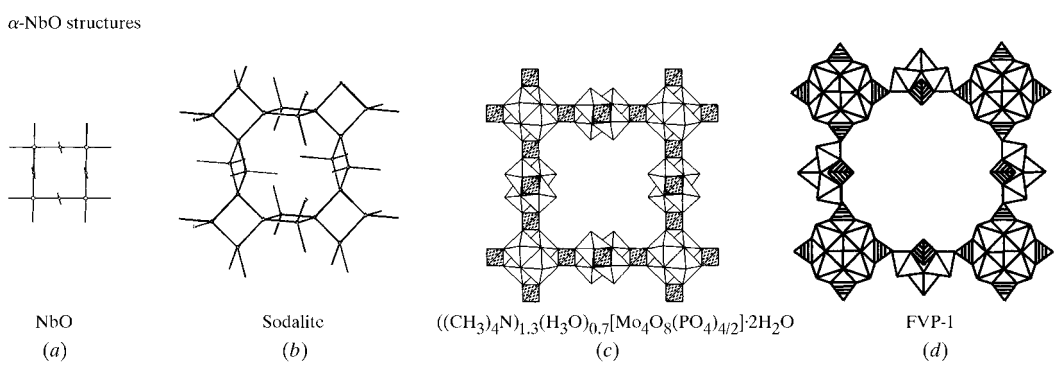

Fig. 4. Parts of (*a*) the NbO net and (*b*) the α-structures of sodalite, (*c*) $((CH_3)_4N)_{1.3}(H_3O)_{0.7}[Mo_4O_8(PO_4)_2]\cdot 2H_2O$, (*d*) and FVP-1. In the α-net of FVP-1, a possible arrangement of the $[V_5O_9]$ groups is shown (FVP-1 is the disordered counterpart of $Cs_3[V_5O_9(PO_4)_2]\cdot xH_2O$).

Table 5. *Survey of α-I-ReO_3 structures with two interpenetrating ReO_3 nets, their groups at the black and white vertices, and the approximate magnification compared with a hypothetical I-ReO_3 structure*

Compound	Groups at the black vertices	Groups at the white vertices	Magnification
Tl_3VS_4	$[VS_4]$	[Tl]	2
$K_2[Zr_6Cl_{15}B]$	$[Zr_6Cl_{12}B]$	[Cl]	2.2
Nb_6F_{15}	$[Nb_6F_{12}]$	[F]	2.2
$Zn_4O(BO_2)_6$	$[Zn_4O]$	$[BO_4]$	2
Helvite: $Mn_8S_2Be_6Si_6O_{24}$	$[Mn_4S]$	$[BeO_4]/[SiO_4]$	2.2
Tennantite: $Cu_{12}As_4S_{13}$	$[Cu_6S]$	$[CuS_4]$	2.7

Table 6. *Survey of α-diamond structures, their groups at the vertices and the approximate magnification compared with the diamond structure*

Compound	Groups at the vertices	Magnification
Diamond: C	[C]	1
Bideauxite: $Pb_4(F,OH)_4[Ag_2Cl_6]$	$[Ag_{4/2}Cl_6]$	4
Harkerite: $Ca_{12}[Mg_4(AlSi_4)(OH)_{16}(BO_3)_4]$	$[Mg_{4/2}(SiO_4)_2(BO_3)_2]$	4.1
Sakhaite: $Ca_2[Mg_2(BO_3)_4](CO_3)_2(H_2O)_{0.72}$	$[Mg_{4/2}(BO_3)_4]$	4.1
Faujasite: $(Na_2,Ca,Mg)_{29}[Al_{58}Si_{134}O_{384}]\cdot 240H_2O$	$[(Si_{0.3}Al_{0.7})_{24}O_{36}O_{24/2}]$	6.9

Table 7. *Survey of α-cristobalite structures, their groups at the black and white vertices, and the approximate magnification compared with the cristobalite structure*

Compound	Groups at the black vertices	Groups at the white vertices	Magnification
SiO_2	[Si]	[O]	1
$[Cd(CN)_2]x\ CCl_4$	[Cd]	[CN]	1.8
$[MnGe_4S_{10}]((N(CH_3)_4)_2$	$[Ge_4S_6]$[Mn]	[S]	2
$[Cd_4S_8](Ph_8)$	$[Cd_4S_6]$	[S]	2.2
$[CuGe_4S_{10}]((C_2H_5)_4N)_2$	$[Ge_4S_6]$	$[CuS_2]$	2.4
$Ag_6B_{10}S_{18}$	$[B_{10}S_{16}]$	[S]	3.6

occupy alternate neighboring vertices (Fig. 3*a*). In the net we are considering below, we do not distinguish between these vertices; hence, the space-group symmetry is raised to $Im\bar{3}m$ and the six vertices are symmetrically equivalent and correspond to Wyckoff site 6(*b*).

In NaCl, both Na and Cl are octahedrally coordinated. Two opposing octahedral corners are lost in NbO and in the NbO net; the result is that both Nb and O are in square-planar coordination. Replacement of each vertex in the NbO (Figs. 3*b* and 4*a*) net by a single four-membered $[Si_2Al_2O_4O_{8/2}]$ ring (S4R) (Figs. 3*c* and 4*b*) yields the crystal structure of the zeolite sodalite (Pauling, 1930; zeolite structure code SOD, see Meier *et al.*, 1996). This topological relation was recognized by Wells (1979, p. 29).

Schindler & Baur (1997) showed that the homeomorphic nets of the following recently synthesized phosphates can be derived by replacing the [S4R] group in the SOD topology by $[V_5O_9(PO_4)_{4/2}]$ or $[Mo_4O_8(PO_4)_{4/2}]$ groups (Figs. 3*d*, 4*c* and 4*d*):

$Na_v[((V^{4+}_{4-w}V^{5+}_{1+w})O_9)(PO_4)_2]\cdot(PO_4)_x\cdot(OH)_y\cdot zH_2O$ (1), with $v = 2.8$–4.0, $w = -0.1$–1.1, $x = 0$–0.2, $y = 0$–2.1 and $z = 7$–10 (named FVP-1 by Schindler *et al.*, 1997);

$Cs_3[V_5O_9(PO_4)_2]\cdot xH_2O$ (Khan *et al.*, 1996), (2);

$((CH_3)_4N)_{1.3}(H_3O)_{0.7}[Mo_4O_8(PO_4)_2]\cdot 2H_2O$, (3) (Haushalter *et al.*, 1989).

In analogy to the SOD topology as an AB_2 structure type, the $[V_5O_9]$ and $[Mo_4O_8]$ groups can be designated as *A* and the $[PO_4]$ groups as *B*. In this way, the $[PO_4]$ groups surround the $[V_5O_9]$ and $[Mo_4O_8]$ groups at the corners of each square-planar unit and connect them with a twist (a relative rotation) of 90°. The resulting chain of square-planar units in the net of SOD topology is termed a *ts* chain (*ts* = twisted square) by Smith (1999). The homeomorphic net of the synthetic phosphate structures was named the α-SOD net by Schindler & Baur (1997). We prefer the homeomorphisms of the FVP-1 and sodalite structures to the original NbO net and thus we refer to them as α-NbO structures because the $[Si_2Al_2O_4O_{8/2}]$, $[Mo_4O_8(PO_4)_2]$ and $[V_5O_9(PO_4)_{4/2}]$ units are located at the vertices of the NbO net. As the groups $[V_5O_9]$ and $[PO_4]$ do not correspond to vertices and edges of the SOD net, terming them α-SOD types, as done by Schindler & Baur (1997), would be misleading in the present context.

Recently, Medrano *et al.* (1998) described the structure of phosphovanadylite. $(Ba_{0.38}Ca_{0.2}K_{0.06}Na_{0.02})$-$[(V_{3.44}Al_{0.46})(OH)_{5.66}O_{2.34}(PO_4)_2]\cdot 12H_2O$ (4).
The structure is similar to that of (3) listed above, but in (4), vanadium(IV) octahedra form a $[V_4O_8]$ group of four edge-connected octahedra. The occurrence of FVP-1 and phosphovanadylite as α-NbO structures is very interesting with regard to the chemistry of vanadium, as $V^{4+}O_n$ and $V^{5+}O_n$ polyhedra occur here as rather different clusters, but reside at the vertices of the same net. One further NbO alpha-structure is $In_{10}S_{18}(HPP)_6(H_2O)_{15}$ (ASU31, HPP = 1,3,4,6,7,8-

Table 8. *Survey of α-cuprite structures, their groups at the black and white vertices, and the approximate magnification compared with the cuprite structure*

Compound	Groups at the black vertices	Groups at the white vertices	Magnification
Cu_2O	[O]	[Cu]	1
$Cd(CN)_2/Zn(CN)_2$	[Cd]/[Zn]	[CN]	1.5
$K_2[B_5O_8]$	$[B_5O_6]$	[O]	2.6
β-$Ca_3Ga_2N_4$	$[Ga_2N_6]$	[N]	3
$(Cu(en)_2)_2[Cu_7Cl_{11}]$	$[Cu_2(Cu_4)_{0.75}Cl_5]$	$[CuCl_3]$	3
δ-GeS_2	$[Ge_4S_6]$	[S]	3.2
$K_2[Pd(Se_4)(Se_6)]$	[Pd]	$[Se_4]/[Se_6]$	3.75
$[Sn_{10}S_{18}O_4](HN(CH_3)_3)_4$	$[Sn_{10}S_{16}O_4]$	[S]	4.1
$[In_{10}S_{18}]((CH_3)_2NH_2)_6$	$[In_{10}S_{16}]$	[S]	4.1
$[Cd_{17}S_4(SCH_2CH_2OH)_{26}]$	$[Cd_{17}S_2(SCH_2CH_2OH)_{26}]$	[S]	6

Table 9. *Survey of several other α-structures, their groups at the white and black vertices, and the approximate magnification compared with the structure type*

Compound	Structure type	Group at the black vertices	Group at the white vertices	Magnification
$(C_6H_{14}N_2)[MnGe_4S_{10}]$	Li-A(BW)	[Mn]/$[Ge_4S_6]$	[S]/[S]	1.8
$[Cd(CN)_2]\cdot x Bu^n_2O\cdot yH_2O)$	Tridymite	[Cd]	[CN]	1.8
[CdHg(CN)$_4$(en)]	PtS	[Cd][Hg]	[CN]	2.4
$[Cd(Cd(CN)_3(C_3H_4N_2))_2]\cdot p$-$C_6H_4Me_2$	Rutile	[Cd]	$[Cd(CN)_3]$	2.9
$K_2Cd(CN)_4$	Spinel	[K]	[Cd]/[CN]	1.6
Leucophosphite: $K_2Fe_4(OH)_2(H_2O)_2(PO_4)_4\cdot xH_2O$	I-Fe	$[Fe_4(OH)_2(H_2O)_2(PO_4)_{8/2}]$	$[Fe_4(OH)_2(H_2O)_2(PO_4)_{8/2}]$	2.4
Jagowerite: $Ba[Al_2(OH)_2(PO_4)_2]$	CaF_2	$[Al_2(OH)_2O_{8/2}]$	$[PO_{4/2}]$	1.6
$AlPO_4$-16, $[Al_{20}P_{20}O_{80}]$	CaF_2	$[Al_4P_4O_{12}O_{8/2}]$	$[AlO_{4/2}][PO_{4/2}]$	2.5
Tschörtnerite $Ca_4(K,Ca,Sr,Ba)_3Cu(OH)_8[Si_{12}Al_{12}O_{48}](H_2O)_x$ ($x \geq 20$)	CaF_2	$[(Si,Al)_{48}O_{48}O_{96/2}]$	$[(Si,Al)_{24}O_{24}O_{48/2}]$	5.8

hexahydro-2*H*-pyrimido[1,2-α]pyrimidine; Li *et al.*, 1999), where four $[In_{10}S_{16}S_{4/2}]$ tetrahedra form an [S4R] group similar to the $[(Si,Al)O_{4/2}]$ tetrahedra in sodalite.

The increasing size of the groups placed at the vertices of the NbO net can be clearly seen in Figs. 3(*b*)–(*e*) and 4(*a*)–(*d*). The [S4R] group in sodalite is approximately double, the $[Mo_4O_8(PO_4)_{4/2}]$ group about 3.4 times, the $[V_5O_9(PO_4)_{4/2}]$ group about 3.8 times and the S4R group of $[(In_{10}S_{16}S_{4/2})_4]$ about 8.1 times the size of the square-planar unit in the NbO net (Table 2).

Remarkably, the dense crystal structure of NbO (with a framework density, FD, of 40.2 cations per 1000 Å^3) is based on the same framework topology as the open arrangement of the zeolite sodalite (with an FD of 17 cations per 1000 Å^3) and the more open $[V_5O_9(PO_4)_{4/2}]$ framework of structure (1) (with an FD of 10.2 cations per 1000 Å^3). Compared with the vanadium phosphate frameworks, the extremely open $[(In_{10}S_{16}S_{4/2})_4]$ framework has a 2.4 times larger maximum diameter.

6. The NaCl [4]^{12} and ReO_3 nets and their metastructures

In the NaCl net each vertex is coordinated by six vertices, each of which is also coordinated by six vertices. The octahedra share corners and form chains in all three crystallographic directions (Figs. 5*a* and 5*b*). Placing an S_2 group at each alternate vertex yields the structure of pyrite, FeS_2 (Brostigen & Kjekshus, 1969; Table 3, Fig. 5*c*). The net of primary bonds in SiP_2O_7 has the same topology as the pyrite structure type (Wells, as quoted by Tillmanns *et al.*, 1973). The $[OP_2O_{6/2}]$ group occupies one type of vertex and is connected to six octahedrally coordinated $[SiO_{6/2}]$ groups at the adjacent vertices (Fig. 5*d*). Nishikiori & Iwamoto (1993) described $(H_{31}O_{14})[CdCu_2(CN)_7]$ as a pyrite-like framework where each vertex is replaced by a $[CNCu_2(CN)_{6/2}]$ group (Fig. 5*e*). This $[CNCu_2CN_{6/2}]$ group is isostructural with the $[OP_2O_{6/2}]$ group in SiP_2O_7, but is more extended because of the length of the linear CN group. A larger magnification of the NaCl-type topology occurs in zunyite $[(Si_5Al_{13}O_{20}(OH)_{14})F_4Cl]$ (Baur & Ohta, 1982), where the vertices are occupied by Keggin-molecule-shaped $[AlO_4Al_{12}O_{12/2}(OH)_{14}F_4]$ groups (with a central AlO_4 tetrahedron) and by $[SiO_4Si_4O_{12/2}]$ groups (Table 3, Fig. 5*f*). These are bridged by O atoms and are arranged in the same way as Na and Cl in the NaCl structure. The crystal structure of $AlPO_4$-16 (structure code ASTl; Meier *et al.*, 1996) is intimately related to that of zunyite. It has a unit-cell content of $[Al_{20}P_{20}O_{80}]$ (Bennett & Kirchner, 1991) with $[AlO_4P_4O_{12/2}]$ pentamers as *A* and $[PO_4Al_4O_{12/2}]$ pentamers as *B* (Table 3). The aluminate and phosphate groups form a three-dimensional tetrahedral framework, whereas zunyite has an interrupted tetrahedral framework in which the phosphate groups around AlO_4 (in $AlPO_4$-16) are replaced by AlO_6 octahedra of the Keggin-type molecule in zunyite. Thus, we can view the $AlPO_4$-16 framework as an α-NaCl structure type composed of $[AlO_4P_4O_{12/2}]$ and $[PO_4Al_4O_{12/2}]$ units.

A further homeomorphism of the NaCl net occurs in the structure of zeolite *A*. It is a simple cubic packing of truncated octahedra of composition $[Si_{12}Al_{12}O_{36}O_{24/2}]$ [one truncated octahedron at site (000), Wyckoff position 1(*a*) in space group $Pm\bar{3}m$] joined at the cube faces to form double four-rings (Gramlich & Meier, 1971); this packing is analogous to the arrangement of vertices in the NaCl net (Table 3, Fig. 5*g*).

By adding vertices of degree two to the centres of the edges [$\frac{1}{2}$ 0 0, 0 $\frac{1}{2}$ 0, 0 0 $\frac{1}{2}$, Wyckoff site 3(*d*), in $Pm\bar{3}m$], we obtain the ReO_3 net with hexavalent black vertices and divalent white vertices. Connecting the centres of the O atoms at the white vertices yields corner-sharing octahedral chains parallel to all three crystallographic axes (Figs. 6*a*, 6*b* and 7*a*). Schindler & Hawthorne (1999) named these chains *cso*-chains in analogy to the *ts*-chains of the SOD topology. Such a *cso*-chain occurs in the boride framework of synthetic $Ca[B_6]$ (Stackelberg & Neumann, 1932), in which B_2 dimers occur at the white vertices and vacancies occur at the black vertices (Fig. 6*c*).

Two large groups of minerals and their synthetic analogues are homeomorphisms of the ReO_3 net: boracites and pharmacosiderites (Table 4). The chemical compositions of the boracites can be expressed collectively as $M_3[B_4O(BO_4)_{6/2}]X$ (where M = Mg, Fe, Mn and X = Cl, F, I, Br). A core coordination tetrahedron of B around an O atom yields an $[OB_4]$ unit (Fig. 6*e*) which resides at the black vertices. Each of the four B atoms is, in turn, tetrahedrally coordinated by O atoms from the three other borate tetrahedra at the white vertices (Schindler & Hawthorne, 1999). Each tetrahedron at each white vertex shares corners with (and thus bridges) two tetrahedra at the black vertices. This results in the general chemical formula $[(OR_4)(ZO_4)_{6/2}]$. The $[OR_4]$ group is surrounded by six tetrahedra $[(ZO_4)_{6/2}]$, where R is a cation tetrahedrally coordinating an O atom and Z is a cation tetrahedrally coordinated by O atoms. The M cations and X anions fill the pores of the borate framework. The *cso*-chains within the ReO_3 net are formed by the connections provided by the tetrahedra at the white vertices (Figs. 6*e* and 7*c*). Additional examples include a series of recently synthesized zinc phosphates (*e.g.* $Na_3[Zn_4O(PO_4)_3]\cdot xH_2O$ with $[OZn_4]$ at the black vertices and $[PO_4]$ at the white vertices; Harrison *et al.*, 1996).

In pharmacosiderite, $K[Fe_4(OH)_4(AsO_4)_{6/2}]\cdot 6H_2O$ (Buerger *et al.*, 1967) and many isostructural compounds the black vertices are occupied by a distorted cube composed of four octahedrally coordinated M atoms (M = Fe, Al, Ti, Ge, Mo *etc.*) and four O atoms or OH groups: $[M_4(O,OH)_4]$. The four fused octahedral coordinations are completed by O atoms of the $[ZO_4]$ (Z = As, P, Si, Ge) groups at the white vertices, so that $[Fe_4(OH)_4]$ resides at the white vertices and $[AsO_4]$ resides at the black vertices (Figs. 6*d* and 7*b*). The

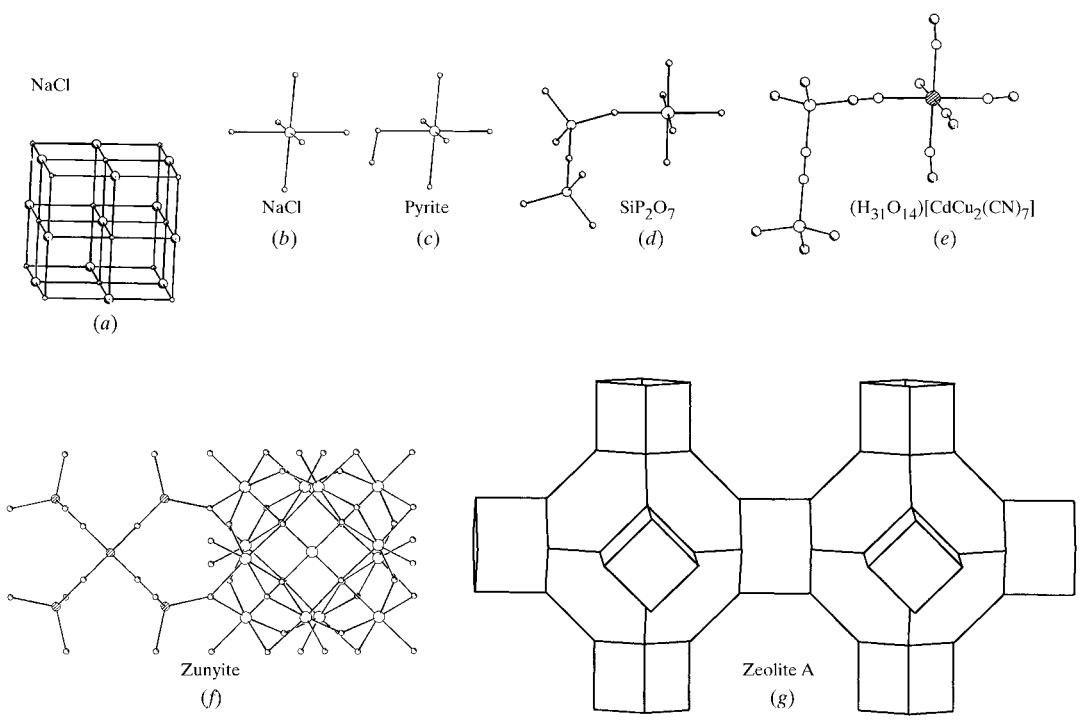

Fig. 5. (*a*) The NaCl net and the different groups of the α-NaCl structures. In all examples, only one group of the six-connected groups around one vertex are completely drawn. For (*b*) NaCl, (*c*) pyrite, (*d*) SiP_2O_7 and (*e*) $(H_{31}O_{14})[CdCu_2(CN)_7]$, one of the octahedrally coordinated vertices is indicated by a larger circle. For (*f*) zunyite, the $[AlO_4Al_{12}O_{12/2}(OH)_{18}]$ group is shown on the right and the $[SiO_4Si_4O_{6/2}]$ group is shown on the left. Two truncated octahedral groups of zeolite A (with all double four-rings) are shown in (*g*).

arrangement in pharmacosiderite is very similar to that in boracite, except that the $[OB_4]$ tetrahedral core group is replaced by an $[M_4(O,OH)_4]$ group. The central core in pharmacosiderite resembles the $[Mo_4O_8]$ unit in $((CH_3)_4N)_{1.3}(H_3O)_{0.7}[Mo_4O_8(PO_4)_{4/2}]\cdot 2H_2O$ (Haushalter *et al.*, 1989); however, the $[Mo_4O_8]$ group is square-planar connected, whereas the pharmacosiderite unit is octahedrally connected.

Another mineral with the ReO_3 topology is sulvanite Cu_3VS_4 (Pauling & Hultgren, 1932). The $[VS_4]$ tetrahedra at the black vertices are octahedrally coordinated by [Cu] groups at the white vertices (Table 4). The cyano complexes $K_2Fe^{2+}[Fe^{2+}(CN)_6]$, $KFe^{3+}[Fe^{2+}(CN)_6]$, $Fe^{3+}[Fe^{3+}(CN)_6]$ and $Fe_4[Fe(CN)_6]_3(H_2O)_{14}$ (Keggin & Miles, 1936; Buser & Ludi, 1972) are ReO_3 alpha structures with [Fe] atoms at the black vertices and [CN] groups at the white vertices. In $Fe(NH_3)_6[Cu_8S(SbS_4)_{6/2}]$ (Schimek *et al.*, 1997), the black vertices are occupied by $[SCu_8]$ units which contain eight fused CuS_4 tetrahedra that share a central S ligand; the Cu atoms are arranged as a cube around S. The white vertices are occupied by $[SbS_4]$ groups (Figs. 6*f* and 7*d*, Table 4) and the $Fe(NH_3)_6$ cations fill the pores of the framework.

Thus, the topology of the ReO_3 net is conformable with a variety of units of very different chemical composition and geometry, and with sizes ranging from four atoms in ReO_3 to 24 atoms in $Fe(NH_3)_6[Cu_8S(SbS_4)_{6/2}]$ (Schimek *et al.*, 1997; Table 4).

7. Interpenetrating NaCl net (4)[12] and the ReO_3 nets and their metastructures

Some structures with such interpenetrating nets were described by Batten & Robson (1998); in Tables 5–8, we show additional structures with larger clusters and groups at the black and white vertices.

A net with two interpenetrating ReO_3 nets (I-ReO_3 net) can be visualized as an arrangement of I-centered cubes with black vertices at $(\frac{1}{2}\,\frac{1}{2}\,\frac{1}{2})$ that are not connected to the vertices at (0 0 0) (Fig. 8*a*). This yields an overall symmetry of $Im\bar{3}m$, in contrast to the space-group symmetry $Pm\bar{3}m$ of the ReO_3 net.

A simple homeomorphism of two interpenetrating ReO_3 nets occurs in $AgTe_3$ (Range *et al.*, 1982) with Ag at the black vertices and Te at the white vertices. Further I-ReO_3 alpha structures are several Zr and Nb halo-

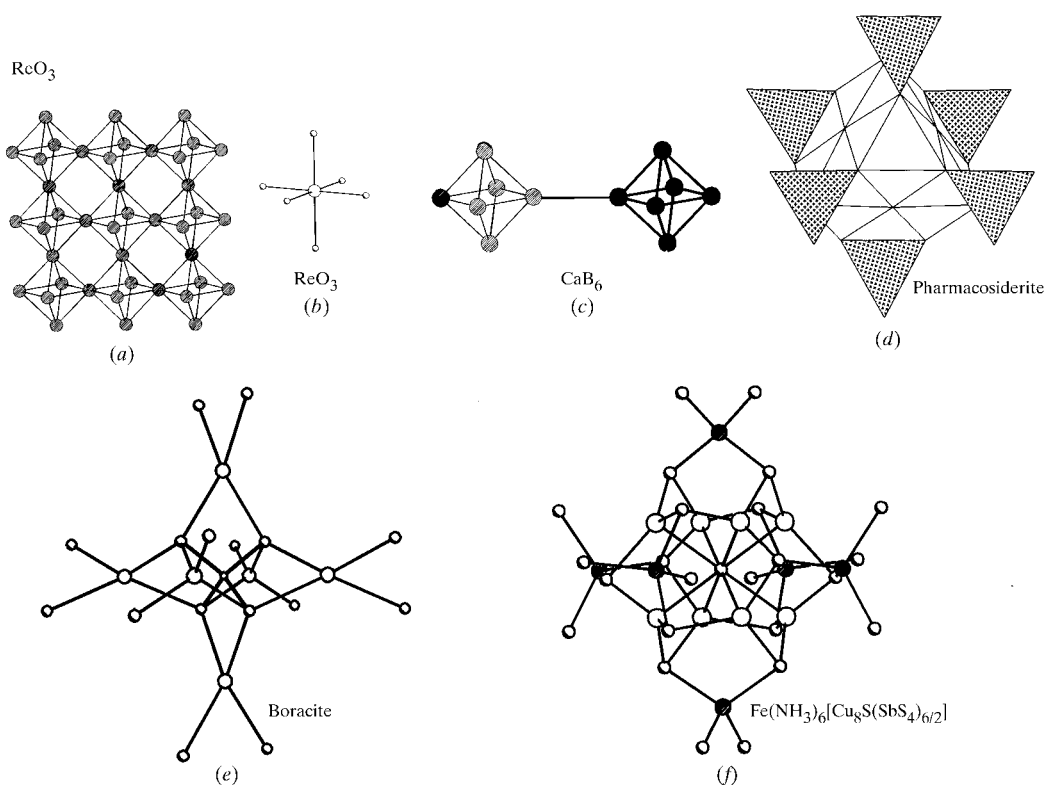

Fig. 6. A slice of (*a*) the ReO_3 structure and the groups of the α-ReO_3 structures; the central Re atoms in the ReO_3 octahedra have been omitted for clarity. (*b*) shows the ReO_3 octahedron and (*c*) a part of the CaB_6 structure. (*d*) The $[M_4(O,OH)_4][TO_4]_{6/2}$ group of pharmacosiderite is shown as four fused octahedra surrounded by an octahedral arrangement of six tetrahedra. (*e*) The central $[OB_4]$ group at the black vertices of the ReO_3 net is emphasized by heavier drawn lines, other O atoms at the black and white vertices have been omitted for clarity, and the B atoms at the white vertices are shown as large circles. Finally, the $[Cu_8S]$ group (at the black vertices) and the $[SbS_4]_{6/2}$ groups (at the white vertices) in $Fe(NH_3)_6[Cu_8S(SbS_4)_{6/2}]$ are shown in (*f*).

genides and Tl_3VS_4 (Vlasse & Fournes, 1978). In $[VS_4][Tl]_{6/2}$, $[VS_4]$ tetrahedra are octahedrally coordinated by [Tl] groups (Table 5). The same topology was described by Schäfer *et al.* (1965) for $[Nb_6F_{12}][F]_{6/2}$ and by Ziebarth & Corbett (1988) for $K_2[Zr_6Cl_{12}B][Cl]_{6/2}$ with $[M_6L_{12}]$ groups (M = Nb, Zr; L = Cl, F) rather than $[VS_4]$ tetrahedra at the black vertices and $[Cl]_{6/2}$ or $[F]_{6/2}$ rather than $[Tl]_{6/2}$ groups at the white vertices (Table 5).

Replacement of the white vertices in the interpenetrating ReO_3 nets by a single four-ring of tetrahedra yields an arrangement of sodalite cages filled by six-valent black vertices (Fig. 8*b*). This arrangement occurs in $Zn_4O(BO_2)_6$ (Smith *et al.*, 1961; Bondareva *et al.*, 1978), where $[BO_{4/2}]$ groups have the same bond topology as the TO_4 aluminosilicate tetrahedra in the zeolite sodalite. The $[Zn_4O]$ group is inside the cage at the black vertex, surrounded by 24 $[BO_{4/2}]$ groups (Fig. 8*c*). The $[Zn_4O]$ group corresponds to the encapsulated NaCl in the sodalite cages. A homeomorphism between $Zn_4O(BO_2)_6$ and the sodalite net does not exist because the $[Zn_4O]$ group does not occupy a vertex in the sodalite net. The $[Zn_4O]$ group is analogous to the $[Zn_4O]$ and $[B_4O]$ groups in boracite and $Rb_3[Zn_4O(PO_4)_3]\cdot 3.5H_2O$. The structures of helvite $Mn_8S_2Be_6Si_6O_{24}$ (Hassan & Grundy, 1985) and tennantite $Cu_{12}As_4S_{13}$ (Pauling & Neumann, 1934) may also be described in this way. In the structure of helvite, $[Mn_4S][Be_3O_6Si_3O_6]$, the $[Mn_4S]$ group is at the black vertices and four $[BeO_{4/2}]$ and $[SiO_{4/2}]$ groups are at the white vertices (Table 4). In tennantite, $As_4[Cu_6S][CuS_2]_6$, $[Cu_6S]$ octahedra occur at the black vertices, the four $[CuS_{4/2}]$ groups are located at the white vertices and the As atoms occupy the interstices of the net (Table 5).

8. The diamond ($6_2\cdot6_2\cdot6_2\cdot6_2\cdot6_2\cdot6_2$), zinc blende and cristobalite nets and their metastructures

In the diamond structure, space group $Fd\bar{3}m$, all C atoms are located at four-connected vertices [Wyckoff site 8(*a*) at 1/8 1/8 1/8 and 7/8 3/8 3/8 plus the corresponding face-centered sites; Figs. 1 and 9]. The framework of faujasite (Baur, 1964) and zeolites *X* and *Y* (zeolite structure code FAU; Meier *et al.*, 1996; Fig. 9*d*) can be seen as a diamond net where all vertices are replaced by groups of tetrahedra in the shape of truncated octahedra of

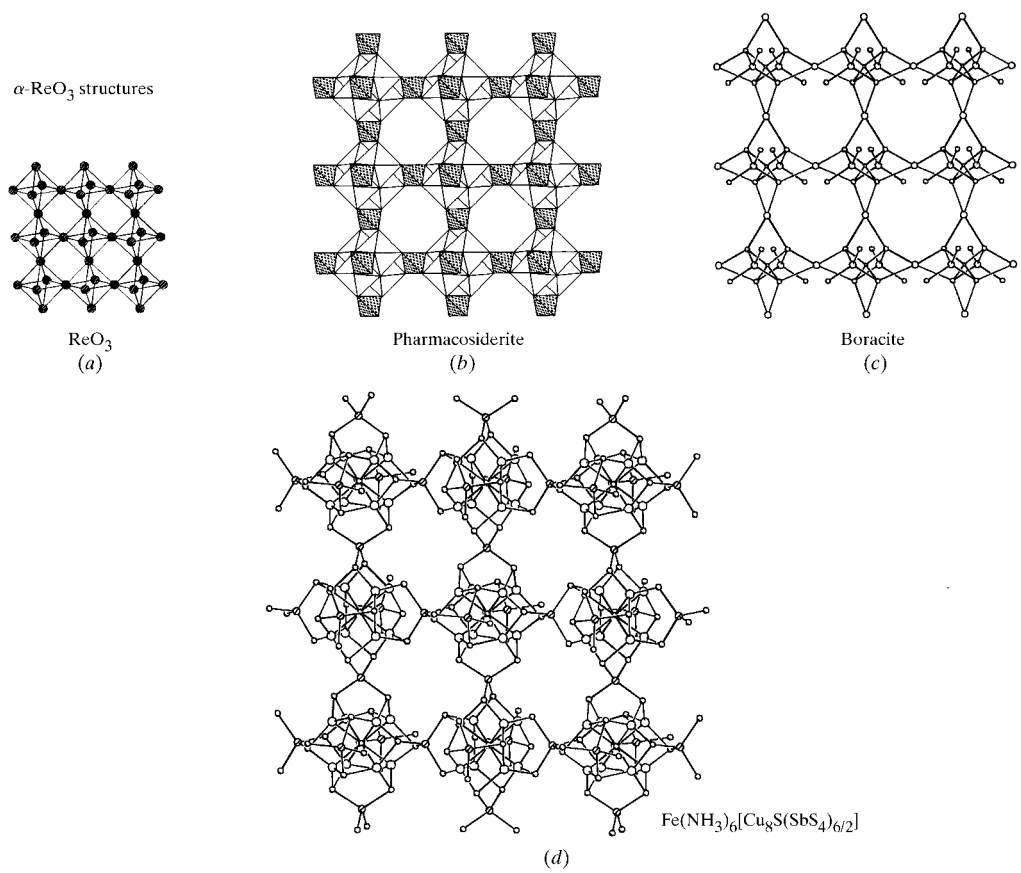

Fig. 7. The nets of (*a*) ReO_3 and the α-structures of (*b*) pharmacosiderite, (*c*) boracite and (*d*) $Fe(NH_3)_6[Cu_8S(SbS_4)_{6/2}]$. In the ReO_3 structure, the central atoms have been omitted for clarity; in the boracite structure, the O atoms of the white vertices have been omitted for clarity. The figure also shows the magnification of the α-structures with increasing size of the groups.

composition $[(Si_{0.3}Al_{0.7})_{24}O_{36}O_{24/2}]$, which are joined at their hexagonal rings (Table 6). A group of condensed octahedra at the vertices of the diamond net occurs in bideauxite $Pb_4(F,OH)_4[Ag_2Cl_6]$ (Cooper *et al.*, 1999). Here, $AgCl_6$ octahedra are fused by corner-sharing into $[Ag_{4/2}Cl_6]$ groups which bond directly to Ag atoms (Fig. 9*b*). A similar case also occurs in harkerite $Ca_{12}[Mg_4(AlSi_4(OH)_{16})(BO_3)_4]$ (Guiseppetti *et al.*, 1977) and sakhaite $Ca_2[Mg_2(BO_3)_4](CO_3)_2(H_2O)_{0.72}$ (Yakubovich *et al.*, 1978; Fig. 9*c*) with $[Mg_{4/2}(SiO_4)_2(BO_3)_2]$ or partly occupied $[Mg_{4/2}(BO_3)_4]$ groups at the vertices of the diamond net. The groups contain MgO_6 octahedra which share corners with BO_3 triangles or SiO_4 tetrahedra (Fig. 9c). Faujasite, bideauxite, harkerite and sakhaite are simple α-diamond structures, even when the vertex of the diamond net is occupied by large polyhedral groups (Table 6).

When the vertices of a diamond net are alternately occupied by Zn and S we obtain the zincblende structure, again with tetrahedral coordination of both Zn and S atoms. Insertion of white vertices of degree two between the four-connected vertices in the diamond net yields the cristobalite net; this homeomorphic SiO_2 structure is an AX_2 structure type with shared O atoms between $SiO_{4/2}$ tetrahedra at the black vertices of the diamond net (Figs. 10*a* and 11, Table 7).

Replacement of the black vertices of the diamond net by [Cd] and the white vertices by a linear cyanide [CN] group (Fig. 10*b*) yields the $Cd(CN)_2{\cdot}CCl_4$ structure (Kitazawa *et al.*, 1988). Further magnification of the cristobalite net occurs when the black vertices are adamantane-like groups of four condensed tetrahedra surrounded by a tetrahedral arrangement of four S atoms at the white vertices, as in the thiolate structure of $[Cd_4S_6][S]_{4/2}(Ph_8)$ (Dance *et al.*, 1987).

Yaghi *et al.* (1994) recognized the relation of $[MnGe_4S_{10}](N(CH_3)_4)_2$ to the diamond net. Here, black vertices are alternately occupied by [Mn] groups and by adamantane-like $[Ge_4S_6]$ groups (Figs. 10*c* and 11), and the $N(CH_3)_4$ ions fill the pores of the framework (see also Achak *et al.*, 1995). Bridging [S] groups at the white vertices link the groups at the black vertices. $[Cu_2Ge_4S_{10}]((C_2H_5)_4N)_2$ (Tan *et al.*, 1995) has a diamond-like framework in which all black vertices are occupied by adamantane-like $[Ge_4S_6]$ groups, which, in turn, are connected and extended by linear $[CuS_2]$ groups at the white vertices (Table 6, Fig. 10*d*). A more extended framework of a cristobalite alpha structure

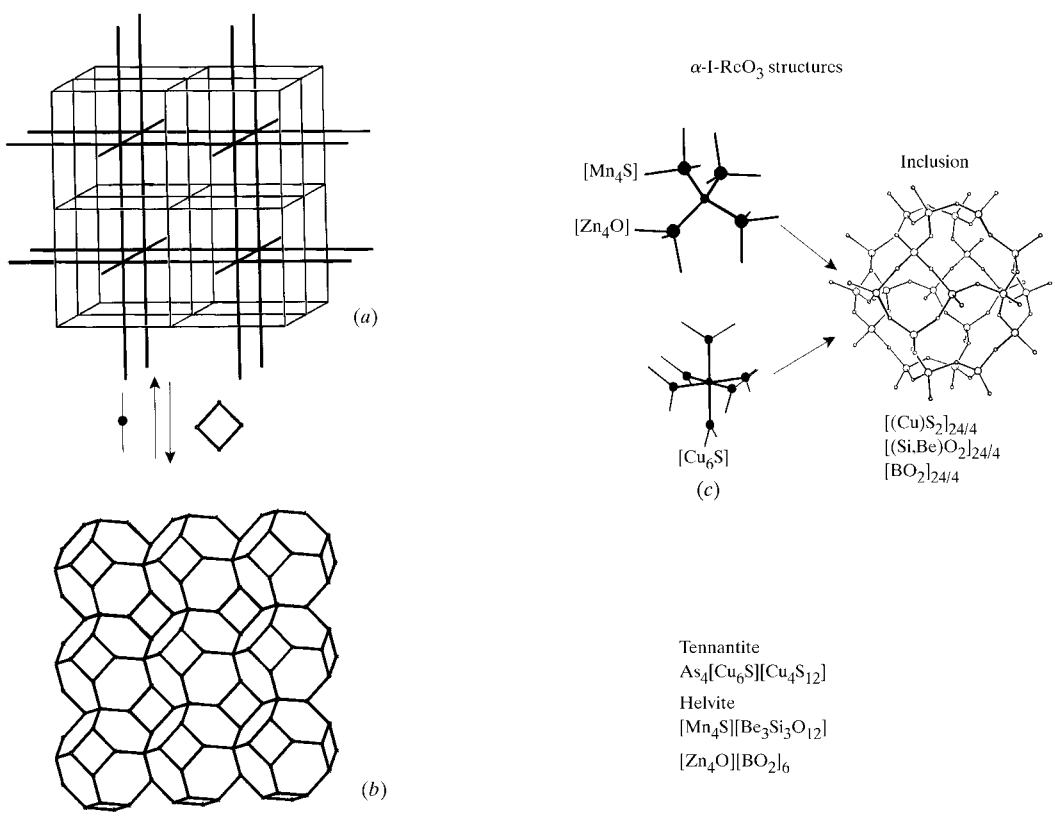

Fig. 8. (*a*) Two interpenetrating ReO_3 nets. One net is emphasized by heavy lines; the two-connected white vertices are omitted for clarity. (*b*) shows the arrangement of sodalite cages, which can be derived by replacing each white vertex by a single four-membered ring. (*c*) Inside the cages reside the black six-connected vertices which can be occupied by $[MnS_4]$, $[Zn_4O]$ or $[Cu_6S]$ groups.

occurs in $AgB_{10}S_{18}$ (Krebs & Diercks, 1984), where $[B_{10}S_{16}]$ tetrahedra at the black vertices are connected by [S] groups at the white vertices.

9. The cuprite, OCu_2 ($6_2{\cdot}6_2{\cdot}6_2{\cdot}6_2{\cdot}6_2{\cdot}6_2$)($6_2{\cdot}6_2{\cdot}6_2{\cdot}6_2{\cdot}6_2{\cdot}6_2$) net and its metastructures

The space group of cuprite, Cu_2O, is $Pn\bar{3}m$. The Cu atoms are at Wyckoff position 4(*c*) (000, $\frac{1}{2}\frac{1}{2}0$, $\frac{1}{2}0\frac{1}{2}$ and $0\frac{1}{2}\frac{1}{2}$) and the O atoms are at position 2(*a*) ($\frac{1}{4}\frac{1}{4}\frac{1}{4}$ and $\frac{3}{4}\frac{3}{4}\frac{3}{4}$); thus, the Cu atoms are in a face-centered arrangement and the O atoms are in a body-centered arrangement. The cuprite structure is homeomorphic with two interpenetrating cristobalite nets with four-coordinated O atoms at the black vertices and two-coordinated Cu^+ atoms at the white vertices (Table 8). The two nets are displaced relative to each other by ($\frac{1}{2}\frac{1}{2}\frac{1}{2}$) and there are no primary bonds between the nets (Figs. 12*a* and 13).

Replacement of the white vertices by linear [CN] groups yields the well known structures of $[Zn(CN)_2]$ (Zhdanov, 1941) and $[Cd(CN)_2]$ (Shugam & Zhdanov, 1945, Fig. 12*b*). In the structure of $K_4[Pd][Se_4][Se_6]$ (Kim & Kanatzidis, 1992), one of the interpenetrating nets consists of Pd atoms tetrahedrally coordinated by chains of four Se atoms, and the other net consists of chains of six Se atoms coordinating Pd (Fig. 12*d*). It is remarkable that, in this instance, the two interpenetrating nets are chemically different and yet are still commensurate (because the net with the longer chains is more folded).

$K[B_5O_4][O_{4/2}]$ (Krogh-Moe, 1965), δ-GeS_2 (MacLachlan *et al.*, 1998) and β-$Ca_3Ga_2N_4$ (Clarke & DiSalvo, 1998) are also complex α-cuprite structures. The corresponding groups at the black vertices are $[B_5O_4]$, $[Ge_4S_6]$ and $[Ga_4N_6]$ clusters which are linked by [O], [S] and [N] groups at the white vertices, respectively (Table 8).

The structure of $[Cu(en)_2]Cu_7Cl_{11}$ (DeBord *et al.*, 1997) can be derived by designating a condensed $[Cu_2(Cu_4)_{0.75}Cl_5]$ group at the black vertices surrounded tetrahedrally by four $CuCl_3$ triangles at the white vertices. The $[Cu_2(Cu4)_{0.75}Cl_5]$ group consists of six $CuCl_4$ tetrahedra (one Cu site is partly occupied) in which an edge-sharing tetrahedral pair shares corners with four tetrahedra; the four tetrahedra form a square-planar arrangement around a common central Cl atom. Two of four $[CuCl_3]$ groups share corners with two $CuCl_4$ tetrahedra of the $[Cu_2(Cu_4)_{0.75}Cl_5]$ group and the other two $[CuCl_3]$ groups share two corners with tetrahedra of the next $[Cu2(Cu_4)_{0.75}Cl_5]$ group (Figs. 12*c* and 13).

Tetrahedrally coordinated large groups at the black vertices also occur in super-tetrahedral clusters such as

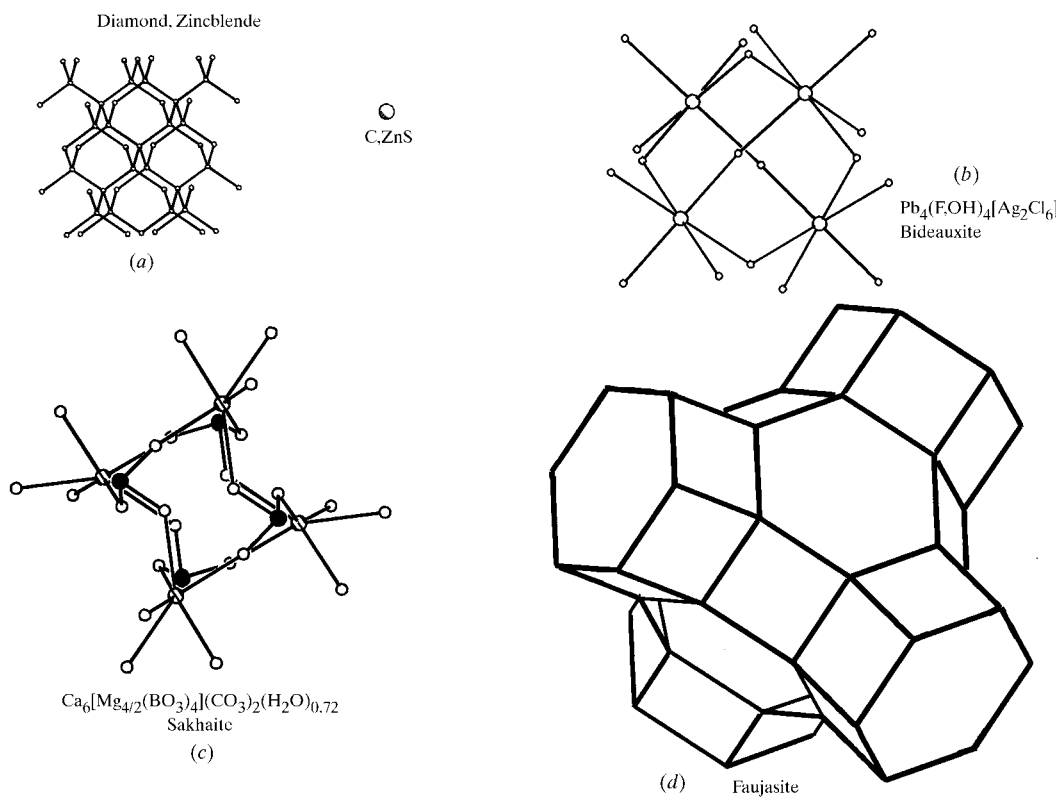

Fig. 9. (*a*) The diamond net and the different groups of α-diamond structures. The four fused ($AgCl_6$) octahedra in the $[Ag_{4/2}Cl_6]$ group of bideauxite are shown in (*b*); the Ag atoms are shown as large circles. In the $[Mg_{4/2}(BO_3)_4]$ group of sakhaite, the (BO_3) triangles are shown as black circles (*c*). (*d*) shows the truncated octahedron of the faujasite structure with its double six-rings.

$[Cd_{17}(SCH_2CH_2OH)_{26}S_2]$ (Vossmeyer *et al.*, 1995), $[In_{10}S_{16}]$ (Cahill *et al.*, 1998) and $[Sn_{10}S_{16}O_4]$ (Parise & Ko, 1994, Table 8). In all three cases, the linking groups at the white vertices are S atoms. The super tetrahedra contain tetrahedrally coordinated Cd, In or Sn atoms and two- or three-coordinated S or O atoms (Fig. 12*e*).

10. Other four-connected nets and their metastructures

10.1. *α-ABW net (4·6·4·6·6·8$_2$)*

Cahill & Parise (1997) described the structure of $(C_6H_{14}N_2)[MnGe_4S_{10}]$ as analogous to the arrangement of (Si,Al) tetrahedra in zeolite Li-A (zeolite structure code ABW; Meier *et al.*, 1996) with alternating [Mn] and $[Ge_4S_6]$ groups at the black vertices, connected by [S] groups at the white vertices. (Table 9).

10.2. *α-Lonsdaleite or α-tridymite net (6$_2$·6$_2$·6$_2$·6$_2$·6$_2$·6$_2$)*

A further three-dimensional four-connected net occurs in $[Cd][CN]_2(x\mathrm{Bu}^n_2\mathrm{O}\cdot y\mathrm{H_2O})$ (x, $y \simeq 0.5$; Kitazawa *et al.*, 1995): the α-tridymite net has [Cd] at the black vertices tetrahedrally coordinated by [CN] at the white vertices (Table 9).

10.3. *α-PtS net (4·4·8$_2$·8$_2$·8$_2$·8$_2$)/(4·4·8$_7$·8$_7$·8$_7$·8$_7$)*

The PtS net occurs in $[CdHg][CN]_4(en)$ (Iwamoto & Shriver, 1972; Table 7) with [Cd] and [Hg] at the black vertices, surrounded by [CN] at the white vertices in square-planar coordination (Table 9).

11. Some nets with six- and eight-connected vertices

In the crystal structure of rutile, TiO_2, ($[4]^2\cdot[6_2]^2\cdot[6]^8$) ($4\cdot[6_2]^2$), a six-connected black vertex is surrounded by white vertices of valence three. The resulting octahedra around the black vertices share edges and corners (Baur, 1956). Kim & Iwamoto (1997) described the crystal structure of $[Cd(Cd(CN)_3(C_3H_4N_2))_2]\cdot p\text{-}C_6H_4Me_2$ as analogous to the rutile structure type (Table 9). The white vertices are occupied by $[Cd(CN)_{6/2}]$ groups, which link to an octahedral arrangement of [Cd] groups at the black vertices (Table 9).

Vertices of valence eight occur in the nets of body-centered iron (Fe at 000 and $\frac{1}{2}\,\frac{1}{2}\,\frac{1}{2}$, space group $Im\bar{3}m$, $[4_3]^{12}\cdot[4]^{12}$) and in CsCl (Table 8). In the framework of zeolite rho, cages of truncated rhombic dodecahedra of composition $[Al_{12}Si_{36}O_{96}]$ correspond to the Fe atoms in body-centered iron: $[Al_{12}Si_{36}O_{72}O_{48/2}]$ (Baur *et al.*,

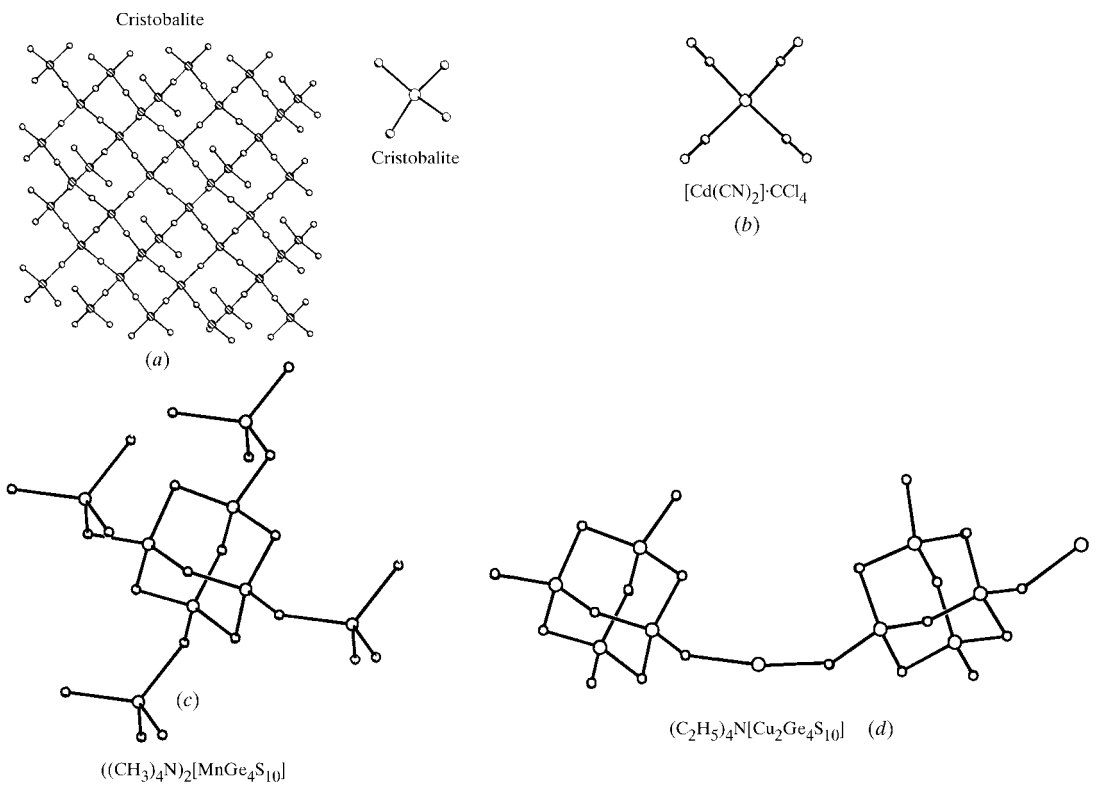

Fig. 10. (*a*) The cristobalite net and the different groups of structures with α-cristobalite topology. In (*b*), the $[Cd(CN)_2]$ group, the C and N atoms are not distinguished. In (*c*) $((CH_3)_4N)_2[MnGe_4S_{10}]$, the adamantane-type $[Ge_4S_6]$ units and the [Mn] group are both located at the white vertices and are tetrahedrally surrounded by [S] groups at the black vertices. In (*d*) $(C_2H_5)_4N[Cu_2Ge_4S_{10}]$, each adamantane-type complex is tetrahedrally coordinated by linear $[Cu^+S_2]$ groups. Two adamantane-type units and one linking $[CuS_2]$ group are shown.

1988). The structures of leucophosphite, $K_2[Fe_4(OH)_2(H_2O)_2(PO_4)_4]\cdot 2H_2O$ (Moore, 1972) and $NH_4[Mo_4O_4(PO_4)_4]\cdot H_2O$ (King *et al.*, 1991) contain $[M_4(O,OH)_4]$ groups (M = Fe, Mo) connected by eight $[PO_4]$ groups. The $[M_4(O,OH)_4]$ group contains an edge-sharing octahedral pair, connected on each side of the common edge to a corner-shared octahedron. The phosphate tetrahedra link two groups together and reside at two-connected vertices at the centres of the edges. However, we did not find an analogous homeomorphic simple structure to the corresponding (eight, two)-connected net. We can consider this as a net of body-centered Fe with $[M_4(O,OH)_4(PO_4)_{8/2}]$ groups at the vertices (Table 9).

In spinel, $MgAl_2O_4$, Mg and Al are tetrahedrally and octahedrally coordinated by O, respectively. Each O atom is coordinated by three Al and one Mg atoms. Therefore, the spinel net contains two different white four-valent vertices, $(6_2\cdot 6_2\cdot 6_2\cdot 6_2\cdot 6_2\cdot 6_2)$ for Mg and $(4\cdot 6\cdot 4\cdot 6\cdot 4\cdot 6\cdot 4\cdot 6)$ for O, and one black six-valent vertex, $([4]^6\cdot[6]^2\cdot[6_2]^4)$. Homeomorphic to the spinel net is $K_2Cd(CN)_4$ (Ziegler & Babel, 1991), with [K] at the black vertices, and [Cd] and the [CN] group at the white vertices $(6_2\cdot 6_2\cdot 6_2\cdot 6_2\cdot 6_2\cdot 6_2)$ $(4\cdot 6\cdot 4\cdot 6\cdot 4\cdot 6\cdot 4\cdot 6)$, respectively.

In the CaF_2 structure type, the white vertices corresponding to F are four-connected and Ca is at eight-connected black vertices $(([4]^{12}\cdot[6_2]^{12})\ ([4]^6))$. A CaF_2 net occurs in jagowerite $Ba[Al_2(OH)_2(PO_4)_{8/2}]$ (Meagher *et al.*, 1974), with condensed octahedral $[Al_2(OH)_2]$ groups at the black vertices, surrounded by eight $[PO_4]$ at the white vertices, forming the corners of a distorted cube (Table 8). Further homeomorphism to the CaF_2 net occurs in the zeolite structures of $AlPO_4$-16 (structure-code AST) and tschörtnerite (Effenberger *et al.*, 1998; structure code TSC). $AlPO_4$-16, described above as an NaCl alpha structure, can also be described as a CaF_2 alpha structure with cubes of $[Al_4P_4O_{12}O_{8/2}]$ composition at the black vertices and $[AlO_{4/2}]$ or $[PO_{4/2}]$ tetrahedra at the white vertices. In tschörtnerite, ideally $Ca_4(K,Ca,Sr,Ba)_3Cu_3(OH)_8[Si_{12}Al_{12}O_{48}](H_2O)_x$ ($x \geq 20$), there are truncated cubo-octahedra (α-cages) of composition $[(Si,Al)_{48}O_{48}O_{96/2}]$ at the black vertices and truncated octahedra (β-cages) of composition $[(Si,Al)_{24}O_{24}O_{48/2}]$ at the white vertices.

12. Examples of (three, four)-, four- and six-connected nets with no simple structural analogues

12.1. *Four-connected net, $(4\cdot4\cdot6\cdot6\cdot8_4\cdot8_4)/(4\cdot4\cdot6\cdot6\cdot10\cdot10)$*

The net of zeolite rho has the long Schläfli symbol 4·4·4·6·8·8 and Smith (1999) showed that the net can be built from *ts*-chains parallel to the diagonal directions [111]. Every second four-membered ring of the rho net is a member of these *ts*-chains. If we replace the single four-rings in the *ts*-chains by four-connected vertices, we obtain a four-connected net with the long Schläfli symbol $(4\cdot4\cdot6\cdot6\cdot8_4\cdot8_4)/(4\cdot4\cdot6\cdot6\cdot10\cdot10)$. As far as we know, there is no homeomorphism between this net and any structure.

Schindler & Baur (1997) showed that the crystal structure of $[HN(CH_2CH_2)_3NH]K_{1.35}$ $[V_5O_9(PO_4)_{4/2}]\cdot xH_2O$ (Khan *et al.*, 1996) has the same overall topology as zeolite rho. The $[V_5O_9(PO_4)_{4/2}]$ groups replace the single four-rings (S4R) in the *ts*-chains of RHO topology. This relation can be visualized when one realizes that four $[V_5O_9(PO_4)_{4/2}]$ groups form a large ring corresponding to the double eight-ring of (Si,Al) tetrahedra in zeolite rho. It is important that we see here the $[V_5O_9(PO_4)_{4/2}]$ units in place of the [S4R] groups, both of which lie on vertices of the $(4\cdot4\cdot6\cdot6\cdot8_4\cdot8_4)/(4\cdot4\cdot6\cdot6\cdot10\cdot10)$ net.

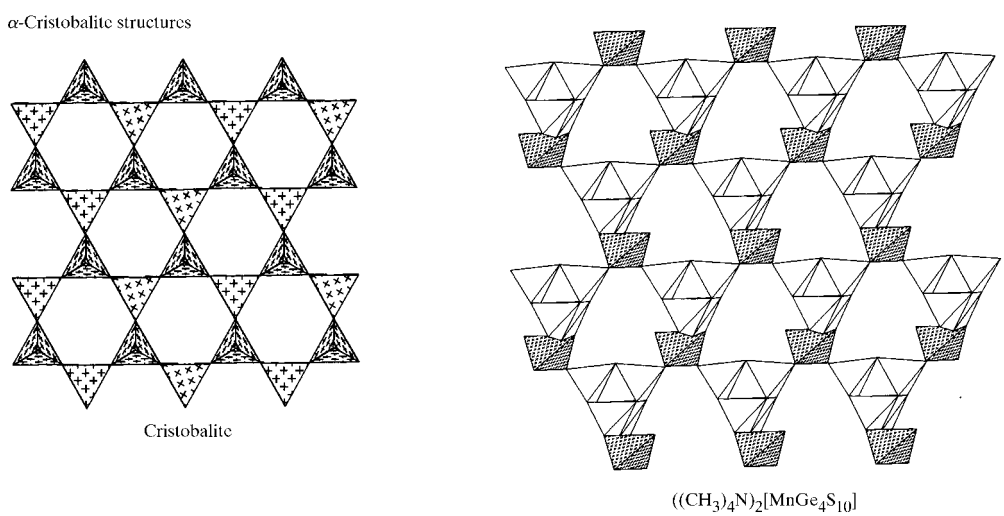

Fig. 11. The cristobalite net and the α-net of $((CH_3)_4N)_2[MnGe_4S_{10}]$. It is apparent that the magnification of the α-structure is due to the replacement of the [Si] group in cristobalite by the larger adamantane-like $[Ge_4S_6]$ group.

12.2. *(Six, two)-connected net; [4]^4·4·4·6$_2$·6$_2$·4·4·6$_2$·6$_2$*

Homeomorphisms to a (six, two)-connected net with squares and hexagons, and overall space-group symmetry $Ia\bar{3}d$, occur in Zr and Nb halogenides of composition $[ML_{12}][L]_{6/2}$, *e.g.* $[Ta_6Cl_{12}][Cl]_{6/2}$ (Bauer & von Schnering, 1968) and $K[Zr_6Cl_{12}C][Cl]_{6/2}$ (Ziebarth & Corbett, 1987). An $[M_6L_{12}]$ cluster occupies the six-valent black vertices and $[Cl]_{6/2}$ groups occupy the two-valent white vertices.

12.3. *(Three, four)-connected net; (8$_3$·8$_3$·8$_3$) (8$_3$·8$_3$·8$_3$·8$_3$·8$_3$·8$_3$)*

A (three, four)-connected net is homeomorphic with the recently synthesized structure of TMA-MGS-2, a metal germanium-sulfide compound in which adamantane-shaped $[Ge_4S_6]$ groups are tetrahedrally surrounded by $[MS_4]$ groups (M = Cu, Co, Ge, Mn; Bedard *et al.*, 1989; Tan *et al.*, 1996) and the $[MS_4]$ groups are three-connected to the adamantane groups. The resulting general formula for the (three, four)-connected α-type structure is $[GeS_6]_3[MS_4]_4$ (TMA).

13. Geometrical and bond-strength requirements

We have shown that many exceedingly complex inorganic crystal structures can be visualized in terms of occupancy of vertices of nets of simple three-dimensional structure types by diatomic groups, polyhedra or larger groups of condensed polyhedra, and are homeomorphic to simple three-dimensional nets. To distinguish them from the simple structure type, we term them α-structures of the corresponding structure type. Atoms, polyhedra or groups of polyhedra can reside at the vertices of these simple nets if they satisfy

(i) the topological requirements;
(ii) the necessary geometrical requirements;
(iii) the bond-strength requirements.

The topological requirements entail having the appropriate number of connectors for a particular net. The geometrical requirements will depend on the shapes of the groups and the flexibility of the structure. Thus, a four-connected vertex cannot be occupied by a triangular group without changing the topology of the bonds. Conversely, each polyhedron or group with four or more free corners could occur at this vertex. A tetrahedral angle of 109.5° does not have to be strictly matched if a

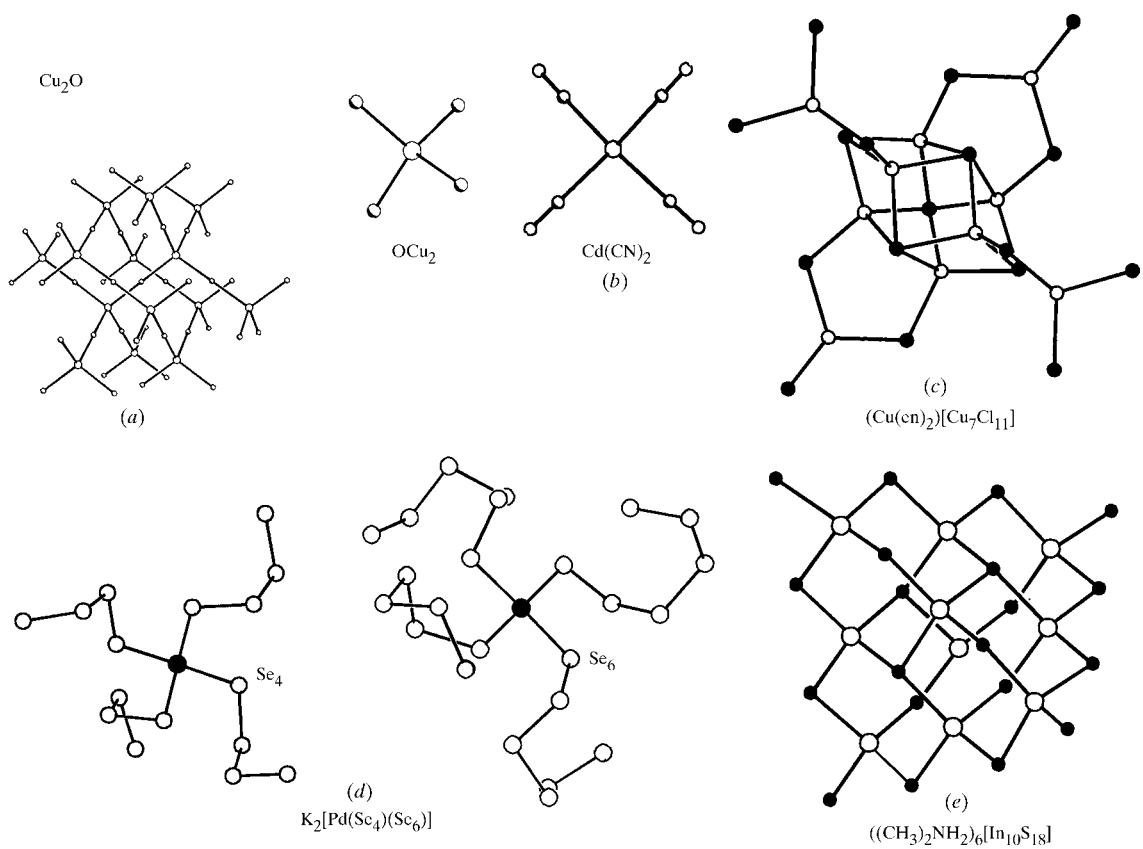

Fig. 12. (*a*) The cuprite net and the α-cuprite structures. Beginning with (*b*), the [CN] group at the white vertices, the size of the groups increases systematically from left to right. In $(Cu(en)_2)[Cu_7Cl_{11}]$ (*c*), six fused $CuCl_4$ tetrahedra form a $[Cu_2(Cu_4)_{0.75}Cl_5]$ group which is tetrahedrally surrounded by four ($CuCl_3$) triangles. (*d*) shows the highly elongated $[Se_4]$ and $[Se_6]$ groups around the [Pd] groups in $K_2[Pd(Se_4)(Se_6)]$. (*e*) The large $[In_{10}S_{16}]$ group is tetrahedrally coordinated by [S] groups in $((CH_3)_2NH_2)_6In_{10}S_{18}$.

structure has the flexibility to absorb a deviation of this angle from the ideal value. If a group has more than the necessary connected corners, additional cations have to balance the bond-strength requirements of the ligands at the free corners.

The bond-strength requirements of different groups can be illustrated by the following examples: in $[Zn_4O][BO_2]_{12/2}$ and $Rb_3[Zn_4O][PO_4]_3{\cdot}3.5H_2O$, the $[Zn_4O]$ group itself is severely underbonded because each Zn requires an additional 1.5 valence units (v.u.) from the three other O atoms of the ZnO_4 tetrahedron: on average, 0.5 v.u. from each O atom. In $[Zn_4O][BO_2]_{12/2}$, these additional O atoms are connected to two B atoms and one Zn atom. In this case, the bond-strength requirements are satisfied because the O atom receives the necessary 1.5 v.u. from the B atoms. Replacement of four $[BO_4]$ groups at the white vertices by groups with higher or lower basicities does not occur in this structure-type. In the α-ReO_3 structure of $Rb_3[Zn_4O][PO_4]_3{\cdot}3.5H_2O$, the corresponding O atoms of the Zn tetrahedra are connected to one Zn and one P atom each (Pauling, 1929; Baur, 1970). They receive only 1.25 v.u. from the P atom, and the additional Rb and H atoms in the interstices have to provide the remaining 0.25 v.u. If the basicity of the units at the white vertices decreases, the acidity of the units at the black vertices and/or the acidity of the interstitial cations must increase; *e.g.* in the boracite structure type $M_3[B_4O][BO_4]_3X$ (M = Mg, Fe, Mn and X = Cl, F, I, Br), the basicity of the $[BO_4]$ groups at the white vertices decreases to 0.75 v.u. In this case, the acidities of the $[B_4O]$ group (0.75 v.u.) at the black vertices and of the interstitial cations ($\sim$0.45 v.u.) increase.

14. Potential for the prediction of crystal structures

Numerous topologies of microporous crystal structures have been successfully predicted based on the systematic search of three-dimensional nets. Among those discussed here, the underlying topologies of the AST-type structure of $AlPO_4$-16 (Bennett & Kirchner, 1991) and of the TSC-type zeolite tschörtnerite (Effenberger *et al.*, 1998) were found by Smith & Bennett (1981). Therefore, it is reasonable to expect that visualizing homeomorphisms between complex inorganic structures and three-dimensional nets can help us to predict new mineral and synthetic inorganic structures. When the bond-strength and geometrical requirements are satisfied, groups such as $[V_5O_9]$, $[Mo_4O_8]$, $[Fe_4(OH)_4]$, $[Zn_4O]$, $[Ge_4S_6]$, [CN] and $[In_{10}S_{16}S_{4/2}]$ can occur at the vertices of several other three-dimensional nets. We mentioned, for example, the replacement of square-planar units in *ts*-chains by $[V_5O_9(PO_4)_{4/2}]$, $[Mo_4O_8(PO_4)_{4/2}]$ and $[V_4O_8(PO_4)_{4/2}]$ groups. The following three-dimensional nets contain these *ts*-chains and thus are potential homeomorphic nets for new

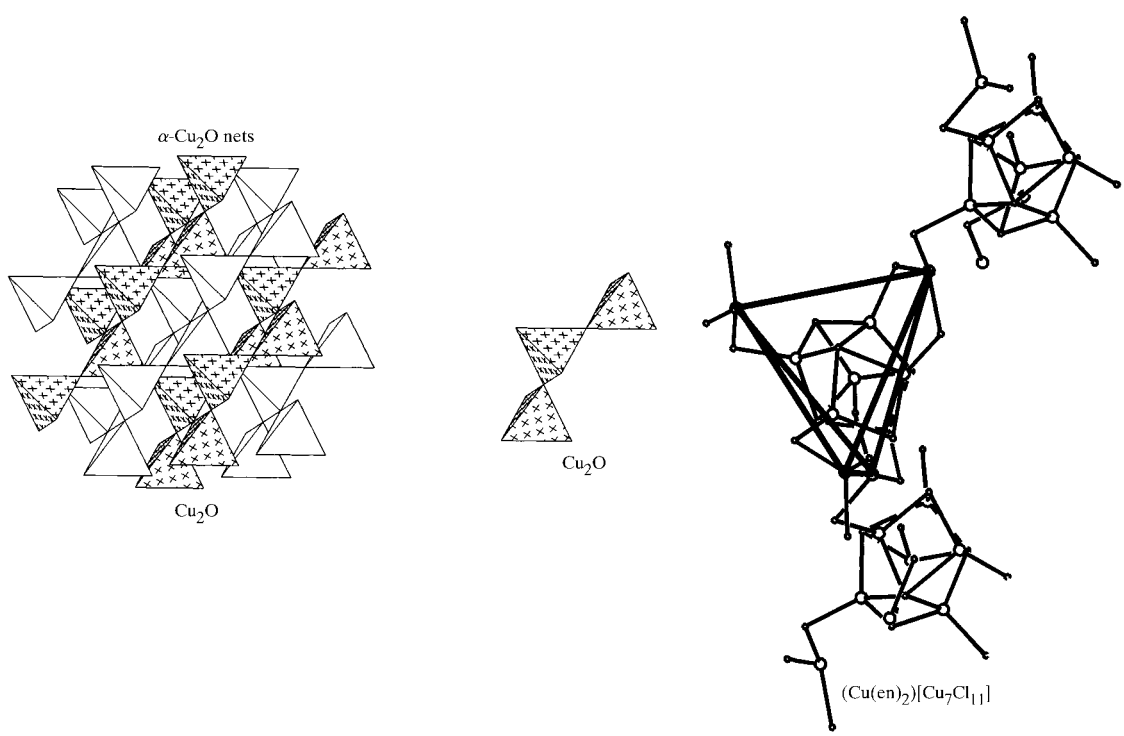

Fig. 13. The structure of cuprite parallel to (110), with crosses marking one of the two nets. Three tetrahedra of the cuprite structure and three $[Cu_2(Cu_4)_{0.75}Cl_5]$ groups tetrahedrally surrounded by $CuCl_3$ triangles are shown in the same orientation. The magnification owing to replacement of the [Cu] and [O] groups by $[Cu_2(Cu_4)_{0.75}Cl_5]$ and $[CuCl_3]$ is clearly apparent.

microporous vanadium or molybdenum phosphate compounds: analcime, TMA-E, gismondine, gmelinite, goosecreekite, laumontite, phillipsite, STA-1, roggianite and yugawaralite (for references, see Meier *et al.*, 1996).

15. Conclusions

Our description of complex structures as simple arrangements of complex clusters is elegant and topologically economical. Furthermore, it reinforces the idea (Hawthorne, 1994, 1997) that nature uses a small number of basic arrangements and produces structural diversity by using a variety of FBBs in these arrangements (FBB = Fundamental Buildings Blocks). The FBBs, in our case the groups located at the vertices of the nets, have to obey the geometrical as well as the bond-strength requirements of the crystal structure.

As homeomorphism to a simple structure-type occurs with larger and larger units at the vertices of the corresponding net, the α-structures expand and can become microporous.

In the organization of the solid state, the same principles can apply at different scales of the units. An even more extreme case of illustrating this is the analogous arrangement of the close-packing of atoms in many crystal structures of metallic elements, of spheres of $SiO_2.nH_2O$ of diameters of $\sim$1500–3500 Å in opal (Jones *et al.*, 1964), of polystyrene beads of a diameter of 0.5 μm in the laboratory (Park *et al.*, 1998) and, finally, of macroscopic objects. Consequently, we might expect to see even larger extended frameworks than have been observed to date.

This work was supported by Natural Sciences and Engineering Research Council of Canada grants to FCH. We thank two anonymous referees for thorough reviews of the original manuscript.

References

Achak, O., Pivan, J. Y., Maunaye, M., Louër, M. & Louër, D. (1995). *J. Alloys Compd*, **219**, 111–115.
Akporiaye, D. E. (1994). *Stud. Surf. Sci. Cat.* **84**, 575–582.
Batten, S. R. & Robson, R. (1998). *Angew. Chem. Int. Ed.* **37**, 1460–1494.
Baur, W. H. (1956). *Acta Cryst.* **9**, 515–520.
Baur, W. H. (1964). *Am. Mineral.* **49**, 697–704.
Baur, W. H. (1970). *Trans. Am. Crystallogr. Ass.* **6**, 129–155.
Baur, W. H., Fischer, R. X. & Shannon, R. D. (1988). *Stud. Surf. Sci. Cat.* **37**, 281–292.
Baur, W. H. & Ohta, T. (1982). *Acta Cryst.* B**38**, 390–401.
Bauer, D. & von Schnering, H. G. (1968). *Z. Anorg. Allg. Chem.* **361**, 259–276.
Bedard, R. L., Wilson, S. T., Vail, L. D., Bennett, J. M. & Flanigen, E. M. (1989). *Stud. Surf. Sci. Cat.* **49**, 375–387.
Bennett, J. M. & Kirchner, R. M. (1991). *Zeolites*, **11**, 502–506.
Bondareva, O. S., Egorov-Tismenko, Y. K., Simonov, M. A. & Belov, N. V. (1978). *Dokl. Akad. Nauk SSSR*, **421**, 815–817.
Bowes, C. L. & Ozin, G. A. (1996). *Adv. Mater.* **8**, 13–28.
Bowman, A. L., Wallace, T. C., Yarnell, J. L. & Wenzel, R. G. (1966). *Acta Cryst.* **21**, 843.
Bragg, W. L. (1930). *Z. Kristallogr.* **74**, 237–305.
Bragg, W. L. & Brown, G. B. (1926). *Z. Kristallogr.* **63**, 538–556.
Brostigen, G. & Kjekshus, A. (1969). *Acta Chem. Scand.* **23**, 2186–2188.
Buerger, M. J., Dollase, W. A. & Garaychochea-Wittke, I. (1967). *Z. Kristallogr.* **125**, 92–108.
Buser, H. J. & Ludi, A. (1972). *J. Chem. Soc. Chem. Commun.* p. 1299.
Cahill, C. L., Ko, Y. & Parise, J. B. (1998). *Chem. Mater.* **10**, 19–21.
Cahill, C. L. & Parise, J. B. (1997). *Chem. Mater.* **9**, 807–811.
Carlucci, L., Ciani, G., Proserpio, D. M. & Sironi, A. (1995). *J. Am. Chem. Soc.* **117**, 12861–12862.
Carlucci, L., Ciani, G., Proserpio, D. M. & Sironi, A. (1997). *Inorg. Chem.* **36**, 1736–1737.
Clarke, S. J. & DiSalvo, F. J. (1998). *J. Alloys Compd*, **274**, 118–121.
Cooper, M. A., Hawthorne, F. C., Merlino, S., Pasero, M. & Perchiazzi, N. (1999). *Can. Mineral.* In the press.
Dance, I. G., Garbutt, R. G., Craig, D. C. & Scudder, M. L. (1987). *Inorg. Chem.* **26**, 4057–4064.
DeBord, J. R. D., Lu, Y., Warren, C. J., Haushalter, R. C. & Zubieta, J. (1997). *Chem. Commun.* pp. 1365–1366.
Effenberger, H., Giester, G., Krause, W. & Bernhardt, H.-J. (1998). *Am. Mineral.* **83**, 607–617.
Gramlich, V. & Meier, W. M. (1971). *Z. Kristallogr.* **133**, 134–149.
Guiseppetti, G., Mazzi, F. & Tadini, C. (1977). *Am. Mineral.* **62**, 263–272.
Han, S. & Smith, J. V. (1999). *Acta Cryst.* A**55**, 360–382.
Harrison, W. T. A., Broach, R. W., Bedard, R. A., Gier, T. E., Bu, X. & Stucky, G. D. (1996). *Chem. Mater.* **8**, 691–700.
Hassan, I. & Grundy, H. D. (1985). *Am. Mineral.* **70**, 186–192.
Haushalter, R. C., Strohmaier, K. G. & Lai, F. W. (1989). *Science*, **246**, 1289–1291.
Hawthorne, F. C. (1979). *Can. Mineral.* **17**, 93–102.
Hawthorne, F. C. (1983). *Acta Cryst.* A**39**, 724–736.
Hawthorne, F. C. (1984). *Can. Mineral.* **22**, 245–251.
Hawthorne, F. C. (1985). *Am. Mineral.* **70**, 455–473.
Hawthorne, F. C. (1986). *Can. Mineral.* **24**, 625–642.
Hawthorne, F. C. (1990). *Z. Kristallogr.* **192**, 1–52.
Hawthorne, F. C. (1994). *Acta Cryst.* B**50**, 481–510.
Hawthorne, F. C. (1997). *EMU Notes Mineral.* **1**, 373–429.
Hawthorne, F. C., Burns, P. C. & Grice, J. D. (1996). *Rev. Mineral.* **33**, 41–115.
Iwamoto, T. (1996*a*). *Comprehensive Supramolecular Chemistry*, Vol. 6, *Solid-state Supramolecular Chemistry: Crystal Engineering*, edited by D. MacNicol, F. Toda and R. Bishop, ch. 19, pp. 643–690. Oxford: Pergamon Press.
Iwamoto, T. (1996*b*). *J. Incl. Phenom. Mol. Recognit. Chem.* **24**, 61–132.
Iwamoto, T., Nishikiori, S., Kitazawa, T. & Yuge, H. (1997). *J. Chem. Soc. Dalton Trans.* pp. 4127–4136.
Iwamoto, T. & Shriver, D. F. (1972). *Inorg. Chem.* **11**, 2570–2572.
Jones, J. B., Sanders, J. V. & Segnit, E. R. (1964). *Nature*, **204**, 990–991.
Keggin, J. F. & Miles, F. D. (1936). *Nature*, **137**, 577–578.
Khan, M. I., Meyer, L. M., Haushalter, R. C., Schweitzer, A. L., Zubieta, J. & Dye, J. L. (1996). *Chem. Mater.* **8**, 43–53.

Kim, C. H. & Iwamoto, T. (1997). *Bull. Kor. Chem. Soc.* **18**, 791–793.
Kim, K. W. & Kanatzidis, M. G. (1992). *J. Am. Chem. Soc.* **114**, 4878–4883.
King, H. E. Jr, Mundi, L. A., Strohmaier, K. G. & Haushalter, R. C. (1991). *J. Solid State Chem.* **92**, 1–7.
Kitazawa, T., Kikuyama, T., Takeda, M. & Iwamoto, T. (1995). *J. Chem. Soc. Dalton Trans.* pp. 3715–3720.
Kitazawa, T., Nishikiori, S., Kurodo, R. & Iwamoto, T. (1988). *Chem. Lett.* pp. 1729–1732.
Kniep, R. & Mootz, D. (1973). *Acta Cryst.* B**29**, 2292–2294.
Krebs, B. & Diercks, H. (1984). *Z. Anorg. Allg. Chem.* **518**, 101–114.
Krogh-Moe, J. (1965). *Acta Cryst.* **18**, 1088–1089.
Liebau, F. (1985). *Structural Chemistry of Silicates.* Berlin: Springer Verlag.
Li, H., Laine, A., O'Keeffe, M. & Yaghi, O. M. (1999). *Science*, **283**, 1145–1147.
MacLachlan, M. J., Petrov, S., Bedard, R. L., Manners, I. & Ozin, G. A. (1998). *Angew. Chem. Int. Ed.* **37**, 2076–2079.
Meagher, E. P., Gibbons, C. S. & Trotter, J. (1974). *Am. Mineral.* **59**, 291–295.
Medrano, M. D., Evans, H. T. Jr, Wenk, H. R. & Piper, D. Z. (1998). *Am. Mineral.* **83**, 889–895.
Meier, W. M. (1968). *Molecular Sieves*, pp. 10–27. London: Society of Chemical Industry.
Meier, W. M., Olson, D. H. & Baerloder, C. (1996). *Atlas of Zeolite Structure Types*, 4th ed. London: Elsevier (for entries after 1996 see: http://www.iza-sc.ethz.ch/IZA-SC).
Moore, P. B. (1966). *Am. Mineral.* **51**, 168–176.
Moore, P. B. (1972). *Am. Mineral.* **57**, 397–410.
Moore, P. B. (1974). *Neues Jahrb. Mineral. Abh.* **120**, 205–227.
Moore, P. B. (1975). *Neues Jahrb. Mineral. Abh.* **123**, 148–159.
Moore, P. B. (1984). *Crystallochemical Aspects of the Phosphate Minerals*, edited by J. O. Niagru and P. B. Moore, pp. 155–170. Berlin: Springer-Verlag.
Nishikiori, S. I. & Iwamoto, T. (1993). *J. Chem. Soc. Chem. Commun.* pp. 1555–1556.
O'Keeffe, M. (1995). *Acta Cryst.* A**51**, 916–920.
O'Keeffe, M. & Hyde, B. G. (1996). *Crystal Structures. I. Pattern and Symmetry.* Washington DC: Mineralogical Society of America.
Parise, J. B. & Ko, Y. (1994). *Chem. Mater.* **6**, 718–720.
Park, S. H., Quin, D. & Xia, Y. (1998). *Adv. Mater.* **10**, 1028–1032.
Pauling, L. (1929). *J. Am. Chem. Soc.* **51**, 1010–1026.
Pauling, L. (1930). *Z. Kristallogr.* **74**, 213–225.
Pauling, L. & Hultgren, R. (1932). *Z. Kristallogr.* **84**, 204–212.
Pauling, L. & Neumann, E. W. (1934). *Z. Kristallogr.* **88**, 54–62.
Pauling, L. & Sturdivant, J. H. (1928). *Z. Kristallogr.* **68**, 239–256.
Range, K. J., Zabel, M., Rau, F., von Krziwanek, F. & Panzer, B. (1982). *Angew. Chem.* **94**, 717–718.
Robson, R. (1996). In *Comprehensive Supramolecular Chemistry*, Vol. 6, *Solid-state Supramolecular Chemistry: Crystal Engineering*, edited by D. MacNicol, F. Toda and R. Bishop, ch. 19, pp. 733–755. Oxford: Pergamon Press.
Robson, R., Abrahams, B. F., Batten, S. R., Gable, R. W., Hoskins, B. F. & Lui, J. (1992). *Supramolecular Archictecture*, edited by T. Bein, Symposium Series 499, ch. 19. Washington DC: American Chemical Society.
Schäfer, H., von Schnering, H. G., Niehues, K. J. & Nieder-Vahrenholz, H. G. (1965). *J. Less-Common Met.* **9**, 96–104.
Schimek, G. L., Kolis, J. W. & Long, G. J. (1997). *Chem. Mater.* **9**, 2776–2785.
Schindler, M. & Baur, W. H. (1997). *Angew. Chem. Int. Ed. Engl.* **36**, 91–93.
Schindler, M. & Hawthorne, F. C. (1998). *Can. Mineral.* **36**, 1195–1201.
Schindler, M., Joswig, W. & Baur, W. H. (1995). *Eur. J. Solid State Inorg. Chem.* **32**, 109–120.
Schindler, M., Joswig, W. & Baur, W. H. (1997). *Z. Anorg. Allg. Chem.* **623**, 45–54.
Shugam, E. A. & Zhdanov, G. S. (1945). *Zh. Fiz. Khim.* **19**, 515–518.
Smith, J. V. (1977). *Am. Mineral.* **62**, 703–709.
Smith, J. V. (1978). *Am. Mineral.* **63**, 960–969.
Smith, J. V. (1979). *Am. Mineral.* **64**, 551–562.
Smith, J. V. (1999). *Tetrahedral Frameworks of Zeolites and Other Microporous Materials.* Landolt-Börnstein, Vol. III/14*a*, *Zeolites*, edited by W. H. Baur and R. X. Fischer. Berlin: Springer. Submitted.
Smith, J. V. & Bennett, J. M. (1981). *Am. Mineral.* **66**, 777–788.
Smith, J. V. & Rinaldi, F. (1962). *Mineral. Mag.* **33**, 202–212.
Smith, P., Garcia-Blanco, S. & Rivoir, L. (1961). *Z. Kristallgr.* **115**, 460–463.
Stackelberg, M. V. & Neumann, F. (1932). *Z. Physik. Chem. Abt. B*, **19**, 314–320.
Takéuchi, Y., Haga, N. & Ito, J. (1973). *Z. Kristallogr.* **137**, 380–398.
Tan, K., Darovsky, A. & Parise, J. B. (1995). *J. Am. Chem. Soc.* **117**, 7039–7040.
Tan, K., Ko, Y., Parise, J. B. & Darovsky, A. (1996). *Chem. Mater.* **8**, 448–453.
Tillmanns, E., Gebert, W. & Baur, W. H. (1973). *J. Solid State Chem.* **7**, 69–84.
Vlasse, M. & Fournes, L. (1978). *C. R. Acad. Sci. Ser. C*, **287**, 47–49.
Vossmeyer, T., Reck, G., Katsikas, L., Haupt, E. T. K., Schulz, B. & Weller, H. (1995). *Science*, **267**, 1476–1479.
Wells, A. F. (1954). *Acta Cryst.* **7**, 535–544.
Wells, A. F. (1977). *Three-Dimensional Nets and Polyhedra.* New York: Wiley.
Wells, A. F. (1979). *Further Studies of Three-Dimensional Nets.* Pittsburgh: American Crystallographic Association.
Wells, A. F. (1984). *Structural Inorganic Chemistry*, 5th ed. Oxford University Press.
Yaghi, O. M., Li, H., Davis, C., Richardson, D. & Groy, T. L. (1998). *Acc. Chem. Res.* **31**, 474–484.
Yaghi, O. M., Sun, Z., Richardson, D. A. & Groy, T. L. (1994). *J. Am. Chem. Soc.* **116**, 807–808.
Yakubovich, O. V., Egorov-Tismenko, Y. K., Simonov, M. A. & Belov, N. V. (1978). *Dokl. Akad. Nauk SSSR*, **239**, 1103–1106.
Zhdanov, G. S. (1941). *Dokl. Akad. Nauk SSSR*, **31**, 352–354.
Ziebarth, R. P. & Corbett, J. D. (1987). *J. Am. Chem. Soc.* **109**, 4844–4850.
Ziebarth, R. P. & Corbett, J. D. (1988). *J. Am. Chem. Soc.* **110**, 1132–1139.
Ziegler, B. & Babel, D. (1991). *Z. Naturforsch. Teil B*, **46**, 47–49.
Zoltai, T. (1960). *Am. Mineral.* **45**, 960–973.